

AD-E200678

AFWL-TR-80-58

AFWL-TR
80-58

RAPID RESPONSE DENSITY PROBE FABRICATION AND TESTING

② **LEVEL III**

Robert A. Golobic, PhD

Research, Analysis & Development, Inc
8405 Lakeview Drive
Colorado Springs, CO 80908

February 1981

Final Report

Approved for public release; distribution unlimited

DTIC
ELECTE
S APR 22 1981 D
B

AIR FORCE WEAPONS LABORATORY
Air Force Systems Command
Kirtland Air Force Base, NM 87117

81 3 16 128

AD A098040




This final report was prepared by Research, Analysis, & Development, Inc, Colorado Springs, Colorado, under Contract F29601-78-C-0072, Job Order 317J0828 with the Air Force Weapons Laboratory, Kirtland Air Force Base, New Mexico. Lt Peter D. McQuade (ARLB) was the Laboratory Project Officer-in-Charge.


When US Government drawings, specifications, or other data are used for any purpose other than a definitely related Government procurement operation, the Government thereby incurs no responsibility nor any obligation whatsoever, and the fact that the Government may have formulated, furnished, or in any way supplied the said drawings, specifications, or other data, is not to be regarded by implication or otherwise, as in any manner licensing the holder or any other person or corporation, or conveying any rights or permission to manufacture, use, or sell any patented invention that may in any way be related thereto.

This report has been authored by a contractor of the United States Government. Accordingly, the United States Government retains a nonexclusive, royalty-free license to publish or reproduce the material contained herein, or allow others to do so, for the United States Government purposes.

This report has been reviewed by the Public Affairs Office and is releasable to the National Technical Information Service (NTIS). At NTIS, it will be available to the general public, including foreign nations.

This technical report has been reviewed and is approved for publication.


RICHARD K. DEJONCKHEERE
Captain, USAF
Project Officer


LAWRENCE SHER
Chief, Beam Control Systems Branch

FOR THE DIRECTOR


DEMOS T. KYRAZIS
Colonel, USAF
Chief, Laser Development Division

UNCLASSIFIED

SECURITY CLASSIFICATION OF THIS PAGE (When Data Entered)

REPORT DOCUMENTATION PAGE		READ INSTRUCTIONS BEFORE COMPLETING FORM
1. REPORT NUMBER AFWL-TR-80-58	2. GOVT ACCESSION NO. AD-A098	3. RECIPIENT'S CATALOG NUMBER 240
4. TITLE (and Subtitle) RAPID RESPONSE DENSITY PROBE FABRICATION AND TESTING		5. TYPE OF REPORT & PERIOD COVERED Final Report
		6. PERFORMING ORG. REPORT NUMBER
7. AUTHOR(s) Robert A. Golobic, PhD		8. CONTRACT OR GRANT NUMBER(s) F29601-78-C-0072
9. PERFORMING ORGANIZATION NAME AND ADDRESS Research, Analysis & Development, Inc. 8405 Lakeview Drive Colorado Springs, CO 80908		10. PROGRAM ELEMENT, PROJECT, TASK AREA & WORK UNIT NUMBERS 63605F/317J0828
11. CONTROLLING OFFICE NAME AND ADDRESS Air Force Weapons Laboratory (ARLB) Kirtland Air Force Base, New Mexico 87117		12. REPORT DATE February 1981
		13. NUMBER OF PAGES 84
14. MONITORING AGENCY NAME & ADDRESS (if different from Controlling Office)		15. SECURITY CLASS. (of this report) UNCLASSIFIED
		15a. DECLASSIFICATION/DOWNGRADING SCHEDULE
16. DISTRIBUTION STATEMENT (of this Report) Approved for public release; distribution unlimited.		
17. DISTRIBUTION STATEMENT (of abstract entered in Block 20, if different from Report)		
18. SUPPLEMENTARY NOTES		
19. KEY WORDS (Continue on reverse side if necessary and identify by block number) Air Density Air Flow High Frequency Turbulence Measurement Radiation		
20. ABSTRACT (Continue on reverse side if necessary and identify by block number) A new air density-measuring probe has been manufactured and tested. The measurement technique is based upon measurement of the energy decay of radioactive alpha particles as they traverse through the air. The probe consists of an alpha particle source, a detector, and signal-processing electronics. The system is designed to measure high-frequency (up to 20 kHz) density fluctuations as well as mean density. Testing was performed using a low-speed heated jet.		

(Continued)

UNCLASSIFIED

SECURITY CLASSIFICATION OF THIS PAGE (When Data Entered)

UNCLASSIFIED

SECURITY CLASSIFICATION OF THIS PAGE(When Data Entered)

Block No. 20 (continued)

Accurate mean density measurements were demonstrated. However, noise in the processing electronics prevented accurate unsteady readings.

UNCLASSIFIED

SECURITY CLASSIFICATION OF THIS PAGE(When Data Entered)

TABLE OF CONTENTS

<u>SECTION</u>	<u>PAGE</u>
I INTRODUCTION	3
II THEORY AND DESIGN OF THE ALPHA DENSITY PROBE	5
III PROBE CONFIGURATION	15
IV OPERATION OF ANALOG CIRCUITRY	24
V DIGITAL DATA ACQUISITION SYSTEM	37
VI DESCRIPTION OF SOFTWARE USED IN DENSITY PROBE DATA REDUCTION	47
VII CALIBRATION	59
VIII FREE CONVECTION DENSITY MEASUREMENTS	70
IX HEATED FREE-JET DENSITY FLUCTUATION MEASUREMENTS . .	73
X CONCLUSIONS	81
 REFERENCES	 82
 GLOSSARY	 83

Accession For	
NTIS GRA&I	<input checked="checked" type="checkbox"/>
DTIC TAB	<input type="checkbox"/>
Unannounced	<input type="checkbox"/>
Justification	
By	
Distribution/	
Availability Codes	
Dist	Avail and/or Special
A	

I. INTRODUCTION

This report presents the results of testing of a simple yet versatile probe for the measurement of air density. The technique incorporates a polonium radioactive alpha particle source and a surface barrier detector. The detector measures the residual energy of alpha particles after they have passed from the source to the detector over a known path length. This residual energy is directly related to the density of the medium through which it has just passed. Previous analysis and experiment ^{1,2} has demonstrated the feasibility of this technique but with no particular concern about the rapidity with which such a measurement could be made.

The objective of the work reported herein is to verify the technique in a high frequency measurement situation; in particular, one involving the fluctuating density in a high speed flow field. The frequency of the density measurement with this technique is directly related to the activity of the source. In turn, a source delivering more counts per second to the detector requires the use of high frequency electronics. As discussed herein, new electronics for the processing of these signals had to be developed as part of this effort. In addition, a new microdetector was developed by Ortec of Oak Ridge, TN.

The electronics collect and store the residual energy values for 64 continuous counts. They are then continually summed as each new count occurs. Processing permits event-dependent and time-dependent data acquisition and storage. The data acquisition system computes the mean and

¹Golobic, R. A. and W. J. Honea, Fundamental Experiments of the Alpha Particle Emitter Probe for Time-Resolved Density Measurements in Air, Final Report, AFWL Contract F29601-77-C-0067, 12 December 77.

²Golobic, R. A. and W. J. Honea, "Analysis and Experiment of An Alpha Particle Emitter Probe Capable of Direct Air Density Measurements," AIAA paper no. 78-1199, presented at the AIAA 11th Fluid and Plasma Dynamics Conference, Seattle, WA, July 10-12, 1978.

standard deviation of each 4096 sums and displays the value on a front panel.

The results presented here demonstrate the usefulness of this probe for quasi-steady and unsteady density measurements. The small size of the probe permits measurements in high speed flows with a minimum of disturbance.

Sections II and III describe the theory and design of the probe. Sections IV and V describe the analog and digital hardware. Section VI describes the software used in data analysis and Sections VII, VIII and IX describe the results of calibration and testing.

II. THEORY AND DESIGN OF THE ALPHA DENSITY PROBE

The theory of performance of the alpha particle emitter probe for air density measurements is well developed and presented in detail in references 1 and 2. These results will be summarized here. The basic principle involved is that as alpha particles pass through a medium they lose energy through collisions, and the remaining or residual energy is measured. This residual energy is directly related to the density, composition and the path length through the medium. The probe utilizes polonium 210, a nearly pure alpha particle emitter, for the source, and a surface barrier detector for the transducer to measure the residual energy.

The fundamental relationships between residual energy and density are described in references 1 and 3 and result from the differential ionization relationship. Neglecting relativistic effects, this relationship is

$$\frac{dE}{d(\rho \ell)} = - \frac{D}{E} \ln (BE) \quad (1)$$

In integral form, for a homogeneous medium

$$\rho \ell = \int_{E_0}^{E_r} \frac{E dE}{D \ln (BE)} \quad (2)$$

The quantities D and B have been found to be nearly constant³ and are,

³Friedlander, G., J. W. Kennedy, and J. M. Miller, Nuclear and Radiochemistry, 2nd edition, Chapter 4, John Wiley, 1964.

for air

$$\begin{aligned} D &= 1.145 \text{ (Mev)}^2/\text{mg/cm}^2 \\ B &= 0.01556/\text{Mev} \end{aligned} \quad (3)$$

This equation is valid only for alpha particles of sufficient energy such that they are above the speed of the valence electrons (electron stopping). Practically speaking, this requires that the mean residual energy be above 1.5 Mev. Above this value there will be insufficient lowspeed alpha particles to affect the mean. With D and B constant, equation (2) is directly integrable, the result being

$$\rho \ell = \frac{D}{B^2} \left\{ \ln \left[\frac{\ln(BE_r)}{\ln(BE_0)} \right] \right\} \sum_{n=1}^{\infty} \frac{(-1)^n}{(n \ n!)} \left[(-2 \ln(BE_r))^n - (-2 \ln(BE_0))^n \right] \quad (4)$$

Equation (4) converges so slowly that integration of equation (3) is best accomplished numerically. Independent of the method of integration, the result is basically the same; the measured residual energy directly couples to the $\rho \ell$ product.

The results reported in reference 2 indicate that experimentally derived curve fits to calibration data can be used to relate density and residual energy when the required range in density is narrow. Figure 1 shows such a result taken from reference 2. An accurate least-squares fit to the data is given in the figure. The previous equations clearly indicate the inverse relationship between density and path length. Rewriting the equation in the figure in terms of $\rho \ell$, the result is

$$\rho \ell = 0.934 (E_0 - E_r) 0.847 \quad (5)$$

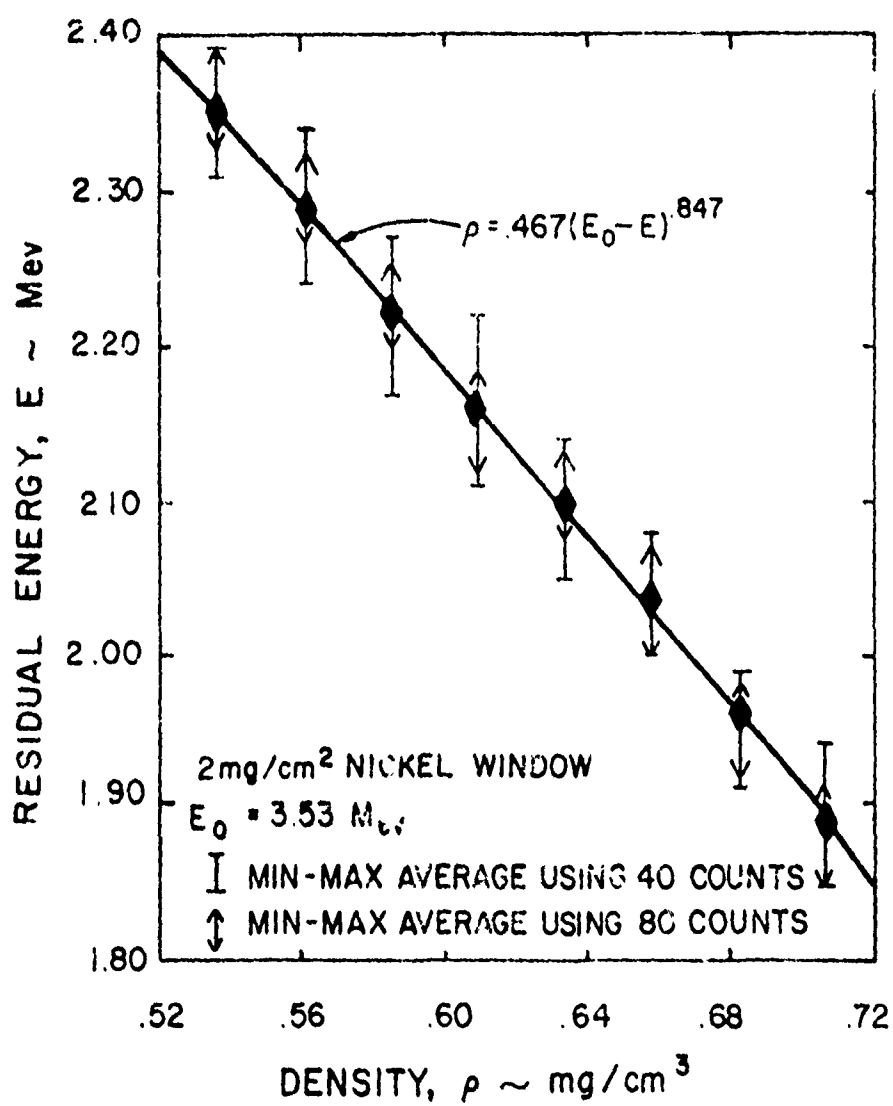


Figure 1. Residual energy versus density including min-max data for various counts and a path length of 2 cm.

In general

$$\rho l = A (E_0 - E_r)^b \quad (6)$$

Equations (5) and (6) are simple relationships between the relevant properties and much can be learned from examining this experimentally derived relationship. First of all, A and b are coefficients to be determined by calibration as they were for equation (5). Calibration can be accomplished by one of two techniques; varying the path length as is done in the experiments reported here, or varying the density as done in the experiments reported in reference 2. Varying the path length provided a simple yet direct technique that can be accomplished without the use of a pressure vessel.

One of the requirements necessary for design of a probe is gained through the examination of the logarithmic derivative of equation (6).

$$\frac{\Delta \rho}{\rho} = \frac{b E_r}{E_0 - E_r} \frac{\Delta E_r}{E_r} \quad (7)$$

The error in the measurement is smallest when the coefficient of $\Delta E_r/E_r$ is the smallest. Clearly, small values of b and E_r will make this coefficient small. The results of reference 2 have demonstrated that b will be largest (near 1) for E_r values near E_0 and smallest (near 0.8) for E_r values near values of 0. The dependence is, however, weak. The value of E_r can be minimized for a fixed density range by making the path length as large as practical. The path length is limited by the following constraints. (1) The path length is restricted to the characteristic dimension within the flow field of interest. (2) The frequency of the

measurement and the required count rate to meet this requirement demand a source size which is determined by the view factor between the source and detector. (3) The residual energy must be no lower than 1.5 Mev to remain in the electron stopping regime as noted earlier in this section.

All these requirements are coupled and they must be compromised in any design. The first requirement must also be tempered with probe diameter requirements. As discussed in detail in the next section, the limiting diameter is governed by the outside diameter of the detector and this is limited to no smaller than 3 mm.

The second requirement is determined by using the view factor shown in figure 2. The diameter, d , of the detector and source are equal.

The third requirement is necessary to insure that standard deviations of the residual energy measurements do not become too large. Nuclear stopping causes the alpha particle to straggle, which results in standard deviations as large as 0.150 Mev. This, of course, requires a larger number of counts to determine the mean to a prescribed accuracy. Another difficulty is contained in the fact that the detector has a prescribed noise width which will affect the measurement at the lowest values. Conventional Ortec detectors have a noise width of 0.016 Mev, while the detectors especially fabricated for this effort have noise widths of 0.006 Mev. These requirements and the past experience reported in reference 2 have led us to the opinion that residual energies of around 2 Mev should be a design goal for the probe, along with path lengths of at least 1 cm to insure adequate undisturbed sampling volume. This latter requirement restricts the use of the density probe for fluctuating measurements to flow fields that have fluctuations of

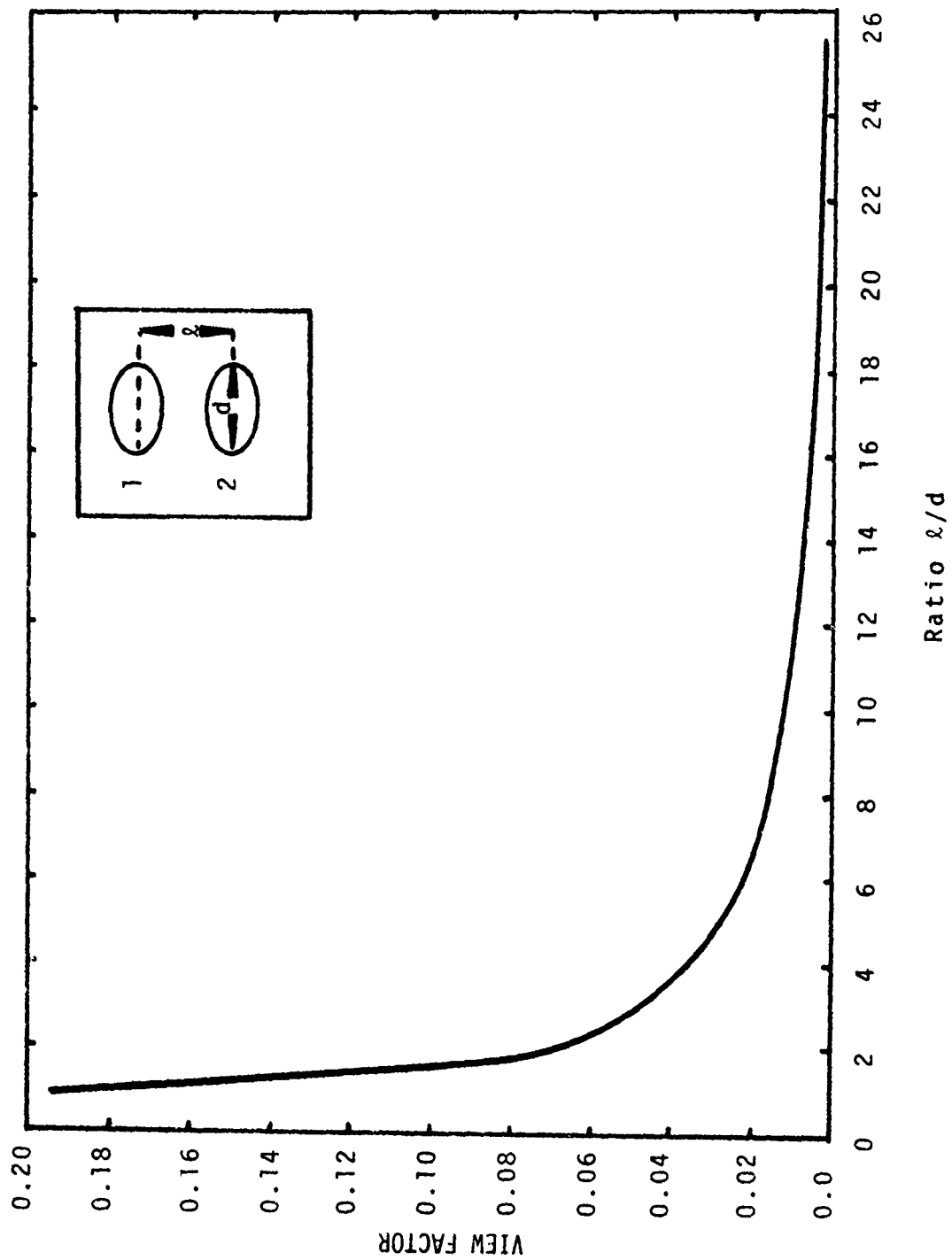


Figure 2. View factor of radiation between parallel discs.

interest which are 1 cm or larger.

Employing the requirements of $\ell \geq 1$ cm and $E_r = 2$ Mev, the condition on E_0 may then be specified once the error requirements and the speed of recording is specified. The results reported in figure 1 clearly demonstrate the fact that the greater the number of counts, the greater the precision of the value of the mean. The expected value of the mean of the residual energy of a group of counts is merely the mean of all the groups of counts plus or minus the standard deviation. Shown in figure 1 are the min-max values which occurred as the results of testing. Quantitatively, the min-max values and the standard deviations are shown in table 1. The number of counts for each mean value is limited by the required sample time. The current goal has been to determine a mean value such that 20 kHz can be resolved. The maximum sample interval to resolve this frequency is 25 μ sec. In 25 μ sec 72 counts could be taken. Since the electronics is best adapted to a binary number, 64 counts has been chosen as the suitable sample size. From the data in table 1, 64

Table 1. Errors resulting in residual energy values when $E_r = 2$ Mev and $\rho\ell = 1.3$ mg/cm² (after reference 2).

Number of counts, N	ΔE_r (Mev) min-max	σ (Mev)
40	0.05	0.014
80	0.03	0.010
160	0.01	0.007

counts yield the following errors

$$\Delta E_r = 0.038 \text{ Mev} \quad (8)$$

$$\sigma = 0.012 \text{ Mev} \quad (9)$$

By using equation (2) the corresponding values of the error in density may also be computed

$$(40 \text{ counts}) \frac{\Delta \rho}{\rho} = 2.1\% \quad (10)$$

$$(80 \text{ counts}) \frac{\Delta \rho}{\rho} = 0.66\% \quad (11)$$

This result indicates the error expected if a probe is configured to operate in the range suggested by figure 1 ($E_0 = 3.53 \text{ Mev}$, $\rho l = 1.3 \text{ mg/cm}^3$, and $E_r = 2 \text{ Mev}$). Since a measurement of density in a fluctuating field is desirable, the min-max error is of most importance. It is also desirable that this error be less than 1%. Equations (7) and (8) can be compared to determine the required value for E_0 . Solving equation (7) for E_0

$$E_0 = E_r + \frac{b E_r}{(\Delta \rho / \rho)} \frac{(\Delta E_r)}{E_r} \quad (12)$$

Using the values from equation (5), $b = 0.847$, equation (8), 1% for $\Delta \rho / \rho$ and $E_r = 2 \text{ Mev}$, the resulting value of E_0 is

$$E_0 = 5.22 \quad (13)$$

Polonium 210 has a maximum value of 5.3 Mev. Window requirements, however, limit the values of E_0 to 4.4 Mev.

Computation of the density/path-length product requires an estimate of the calibration curve. Using the data of reference 2, A and b, the resulting calibration equation is

$$\rho l = 1.16 (4.4 - E_r)^{0.904} \quad (14)$$

For $E_r = 2$ Mev

$$\rho l = 2.56 \text{ mg/cm}^2 \quad (15)$$

The respective density errors are

$$\frac{\Delta \rho}{\rho} = 1.43\% \quad (16)$$

$$\frac{\Delta \rho}{\rho} = 0.45\% \quad (17)$$

As noted in reference 2, several factors within the electronic design can be improved which, in turn, can affect the error associated with the min-max values. Improvements, such as 12-bit analog-to-digital converter and high-speed peak sample and hold is expected to reduce the min-max error to below 1%.

The free stream conditions in the AFWL free-jet wind tunnel are (dome pressure 200 lb/in² g)

$$M_{\infty} = 0.89$$

$$\rho_{\infty} = 1.38 \text{ mg/cm}^3 \text{ (est.)}$$

From equation (15) the required path length is

$$L = 1.86 \text{ cm}$$

Earlier in this section a count rate was specified in order to have a sample rate of 25 μsec . It was also specified earlier that the sum of 64 counts was to occur in 25 μsec . Subtracting 3.5 μsec for overhead time, a count every 336 nsec at the detector must be taken to meet the time interval. The view factor required for a path length of 1.86 cm and a 2 mm active diameter is 0.016. The required average time between alpha particle emissions is then 10.8 nsec. This translates to a required activity of 2.5 mCi. It is important to note that such a path length may be in excess of characteristic length scales of the turbulence present in the stream.

This section has outlined the techniques for design of a density probe. They represent a stringent set of requirements that require unique instrumentation as outlined in the next two sections.

III. PROBE CONFIGURATION

The density probe as designed for these series of experiments has several innovative designs which make it a unique state-of-the-art instrument. The probe, as it was mounted in a wind tunnel test, is shown in figures 3 and 4. The size of the device is best referenced to the 2.54 cm x 10 cm free jet orifice. The vernier slide permits mechanical adjustment of the horizontal and vertical position of the probe. The scales are metric and settings to 0.1 mm are possible. The micrometer barrel, which is also incremented metrically, provides the adjustment of path length. The path length may be adjusted from zero to 3 cm to within 0.1 mm. This path length adjustment, although not originally specified, serves a twofold purpose. First of all, it provides a means of calibration independent of a pressure vessel. This calibration technique is described in Section VII. Secondly, it permits variations so that an optimum path length may be determined experimentally.

The source shown in figures 3 and 4 has been specially fabricated by Isotope Products of Burbank, CA. The vacuum deposition of 20 mCi of polonium on a 2 mm diameter spot represents a state-of-the-art requirement. Several anticipated difficulties, such as internal heating of the polonium and obtaining necessary deposition density without flaking, were not encountered. A cross-sectional view of the source configuration is shown schematically in figure 5. A 1.2 mg/cm² titanium window provides a window for the polonium source. Such a cover is required so that the environment

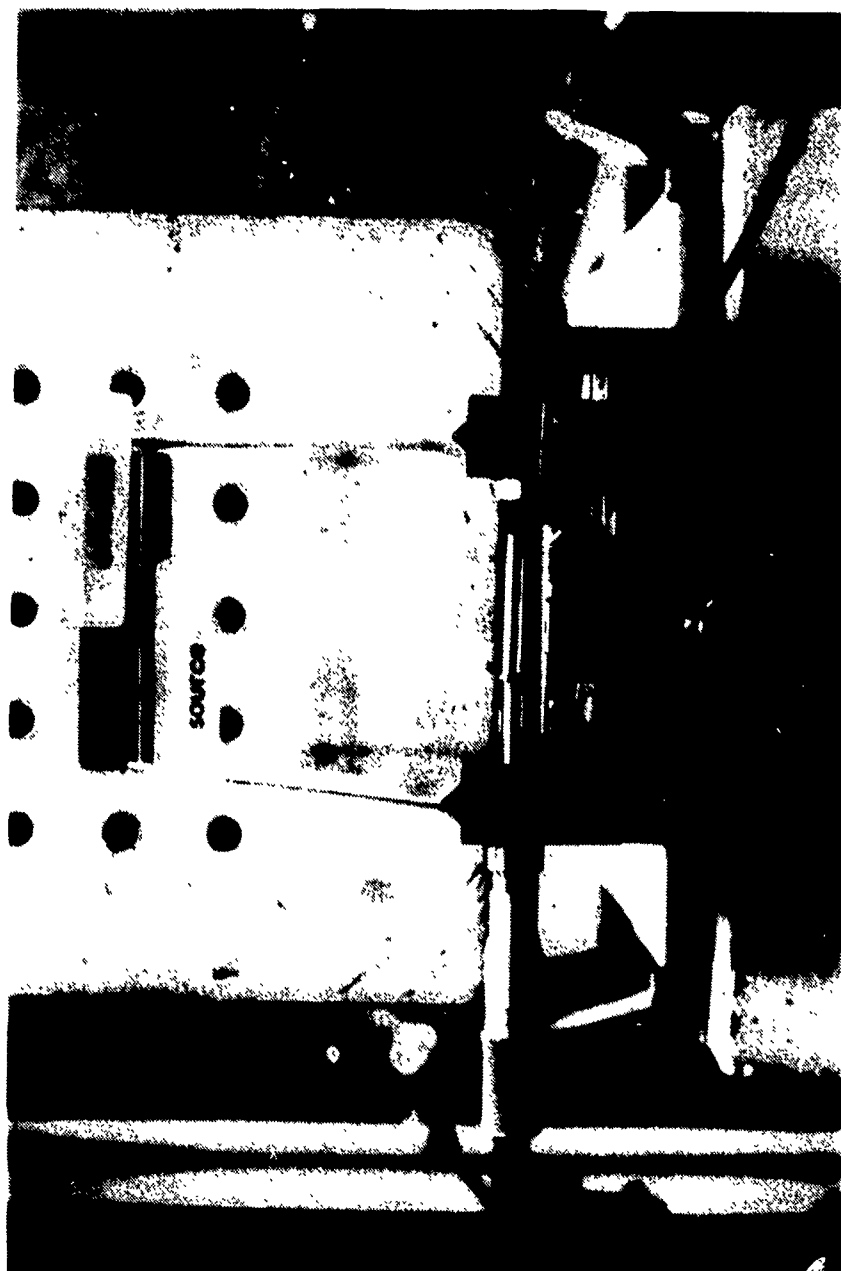


Figure 3. End view of free jet wind tunnel with density probe mounted in place.
The free jet dimensions are 2.54 cm x 7.62 cm.

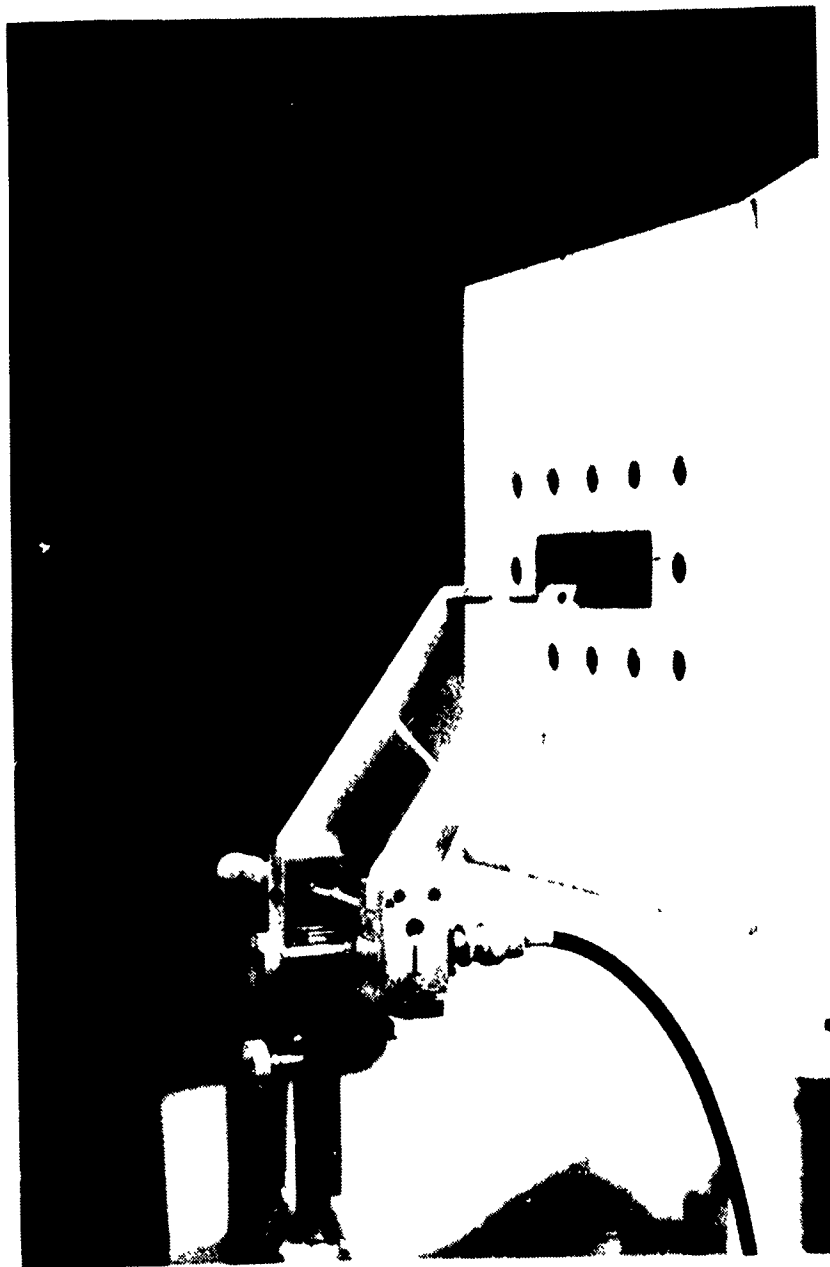


Figure 4. Oblique view of free jet wind tunnel with density probe mounted in place.

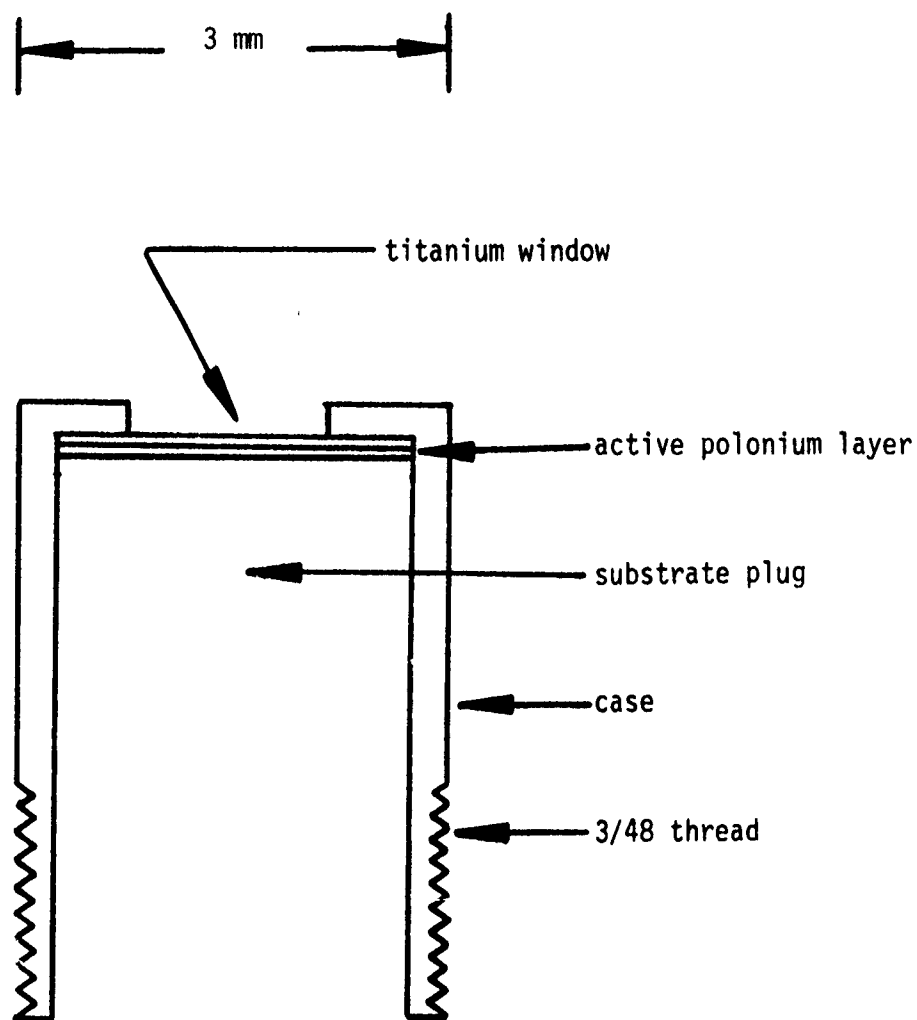


Figure 5. Schematic of polonium α -source fabricated by Isotope Products.

is protected from the danger of the polonium escaping. The window has been found to be quite durable and permits the source to be subjected to relatively harsh environments, e.g., high-velocity flows.

The detector has been specially fabricated by Ortec, Inc. of Oak Ridge, TN. A cross section of the device is depicted in figure 6. This detector has been fabricated in a manner similar to other Ortec standard series surface barrier detectors. The size, however, makes this detector unique. The size also made fabrication an extremely difficult task. The metal case was especially fabricated and gold plated by RAD. Ortec then constructed the detector. The special surface preparations required proved to be extremely difficult and time consuming. A success rate of one in six occurred. The attachment of leads proved to be especially critical in the operation of the detector. The case lead can be connected in a number of ways, but the detector lead requires special attention. The size of the detector prohibits attachment by soldering. Conductive paint was used by Ortec and this proved to be a problem. This method of attachment provides no mechanical or thermal integrity. A heat gun was used in one set of experiments to demonstrate the measurement technique and caused this contact to become irreparably detached.

During wind tunnel testing another detector shook loose. Upon examination, this wire appeared to have broken loose from an aluminum surface without damaging the surface. In attempting to repair this detector, the face was damaged and it was rendered inoperative. It is our opinion that this attachment should have been reinforced with standard epoxy. In addition to these two detectors, a third was damaged in the process of mounting it to the probe.

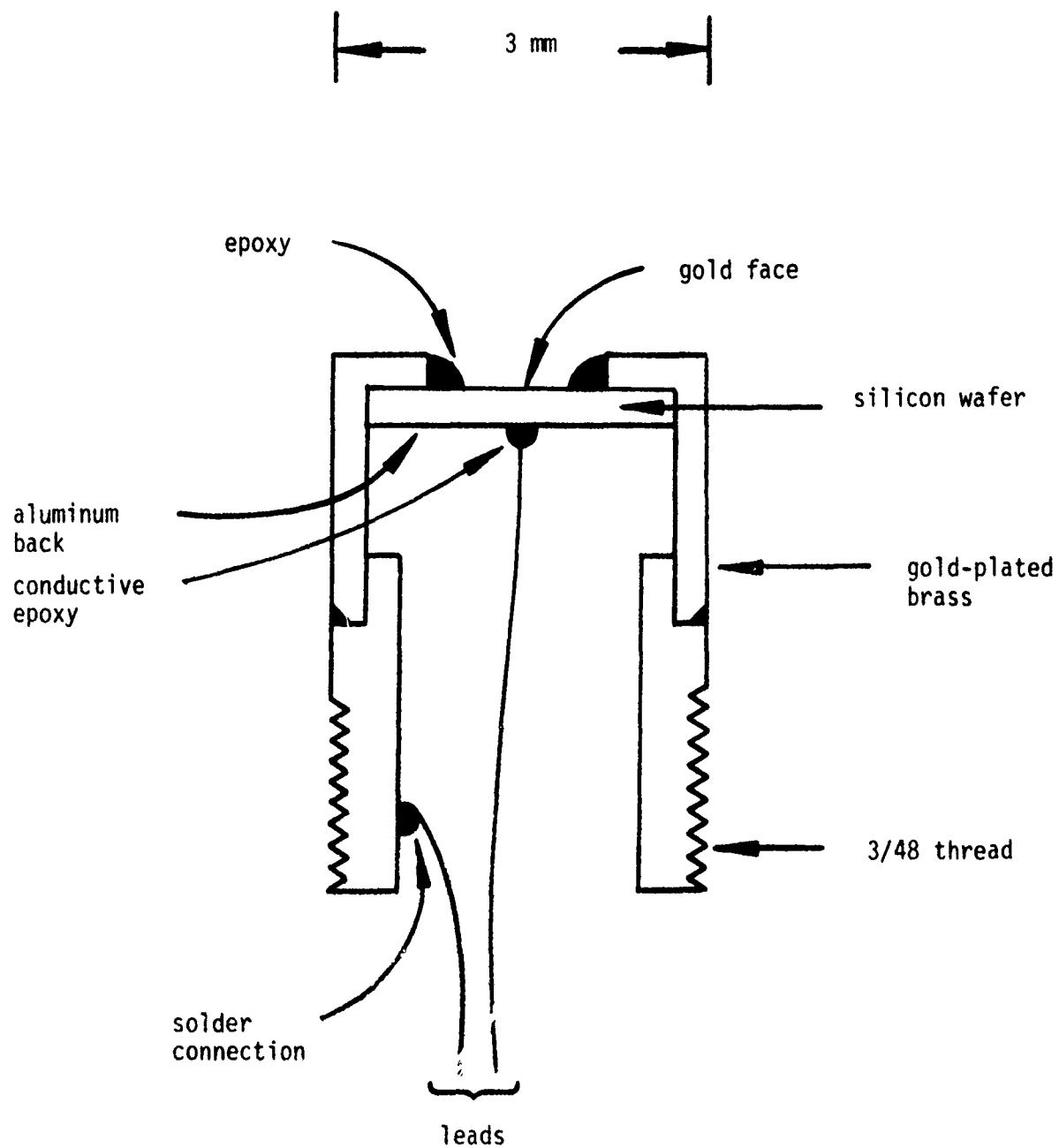


Figure 6. Schematic of specially fabricated detector (fabrication by Ortec).

Another type of detector has also been utilized. It is shown mounted on the probe stand in figures 7 and 8. This detector is the smallest off-the-shelf detector made by Ortec. Here it is shown encapsulated in a brass case with a 2 mm diameter window. The case not only serves as a mount for the detector but also makes the necessary electrical contact.

The leads from the detector form a twisted pair which terminate at the BNC connector. A short (nominally 40 cm) 50 Ω cable then connects the detector to the preamp. Such an arrangement has been found to adequately minimize the noise from the detector.

The vernier slides and the micrometer barrel have proven to be quite adequate. The clearances required for the sliding action, did, however, cause the probe mount to move slightly in the wind tunnel flow. It was therefore not possible to set the position of the probe in the flow as accurately as the vernier slides could be set.

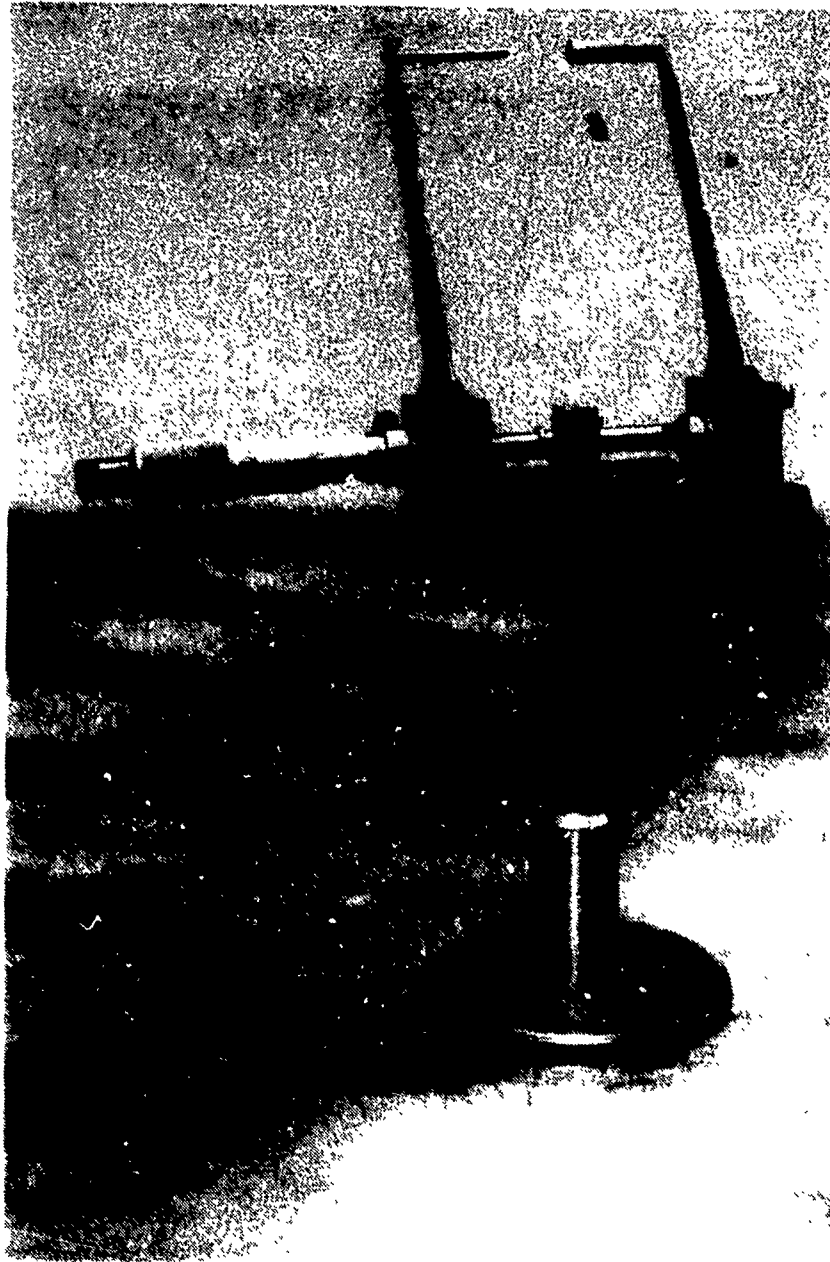


Figure 7. View of probe with large detector installed.

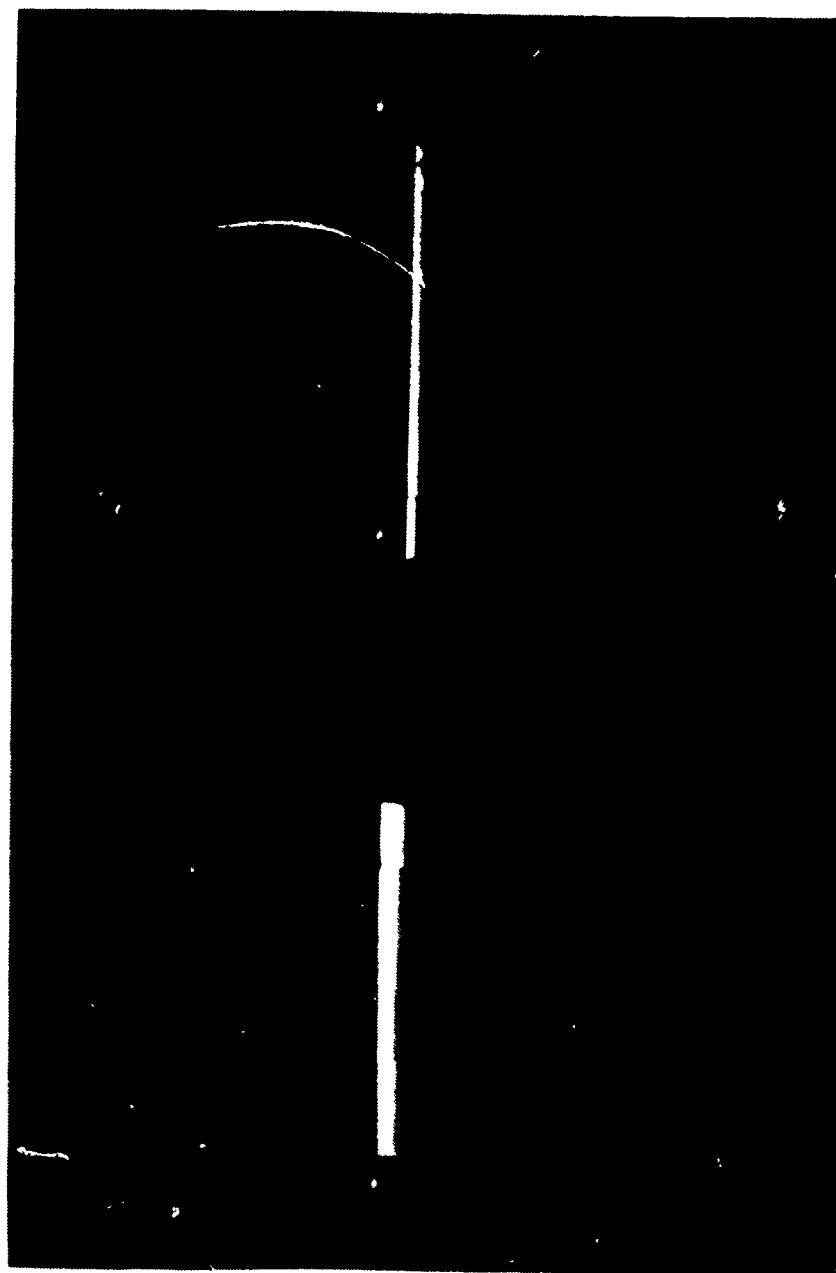


Figure 8. Close-up view of probe with larger detector. Separation distance 2 cm.

IV. OPERATION OF ANALOG CIRCUITRY

The analog circuitry provides for the acquisition and conditioning of the signals corresponding to residual energy. A block diagram of the circuit is shown in figure 9. The purpose of the circuitry is to sum up 64 signals which are each proportional to the energy of a single alpha particle.

When an alpha particle strikes the detector, a charge proportional to the energy of the ionizing radiation is created. The amplifier converts this signal to a low impedance voltage which is also proportional to the energy of the ionizing radiation. The bias potential necessary for proper detector operation is provided in parallel with the amplifier. The output signal from the amplifier has a rise time of 1 to 2 nsec. It has the characteristic step rise and exponential fall with an overall width of 800 nsec. It is limited to a maximum level of 2 volts. Typical valid signals lie in a 0.5 to 1.5 volt range. Typical noise levels are on the order of 0.25 volt.

The pulse signal output from the preamplifier is compared with a prescribed DC level in the discriminator circuit during the rise time. The noise and those pulses which occur at the noise level or below are eliminated. Valid pulses, i.e., those with levels above the discriminator, trigger the clock pulse generator circuit and pass to the sample and hold circuitry. The clock pulse circuitry generates the proper timing pulses to shift the data through the shift registers. It also provides a

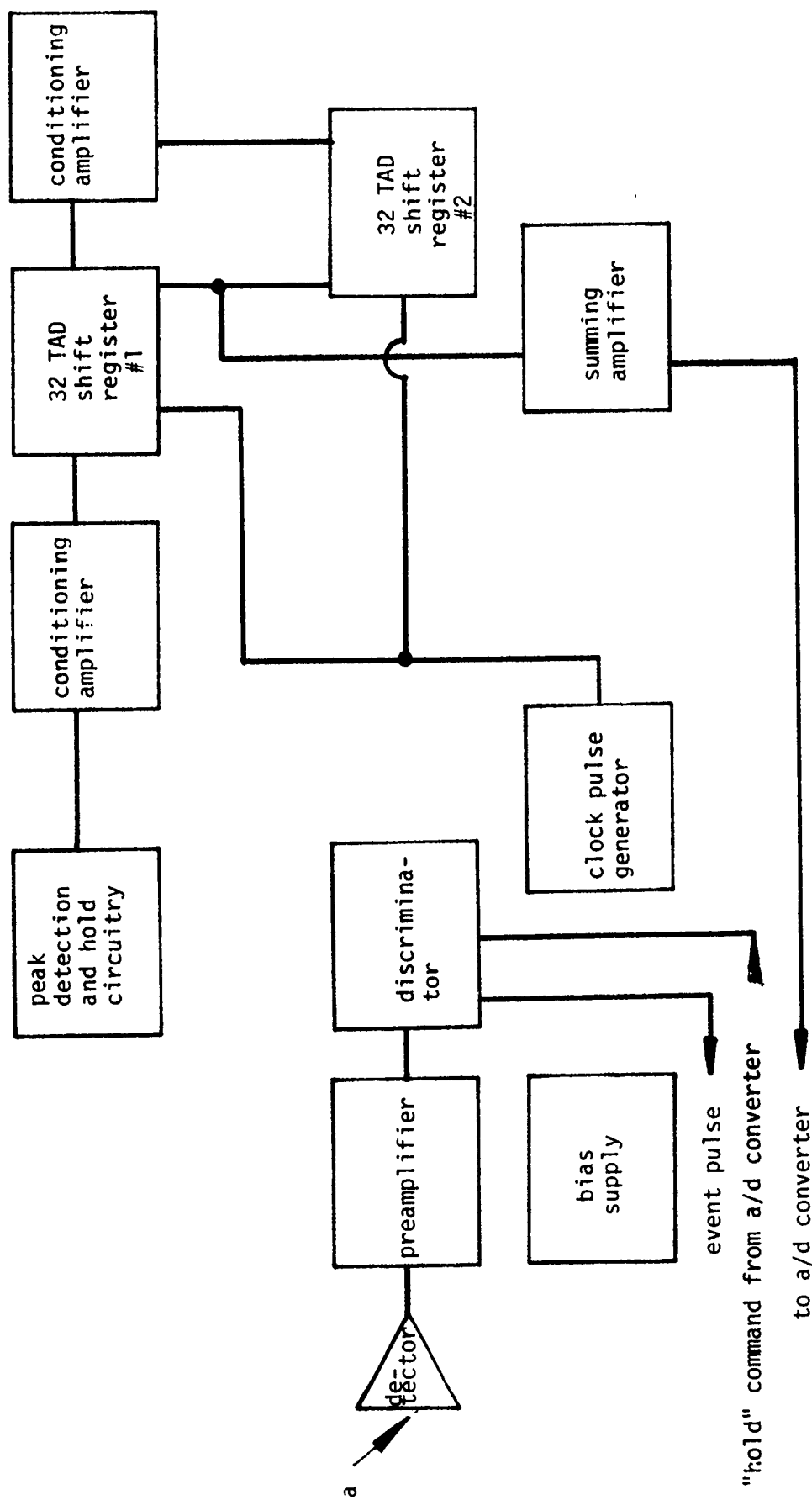


Figure 9. Block diagram of analog circuitry system.

hold on the discriminator to insure that no other pulse is sampled until one is properly clocked. The sample and hold circuitry consists of two sample and hold circuits. Input signals are switched between the two so that each circuit has adequate time to return to a zero level. The sampled signal passes through a conditioning amplifier prior to its input into the shift register to insure that the shift register has an input of proper effect and gain. This entire process occurs in about 300 nsec. The sample and hold circuitry holds a peak for about 200 nsec, and the shift register begins to transfer the signal at 100 nsec after the signal passes through the discriminator. This is coincident with the midway point of the sample and hold signal.

The shift register circuitry is provided for by two Reticon TAD-32 tapped analog delays. Each shift register is capable of holding 32 samples. A signal is shifted sequentially from tap 1 in shift register number one to tap 32. The signal then passes through a conditioning amplifier prior to entry into tap 1 of shift register number two. This insures that the two shift registers are balanced. The 64 shift registers are connected to a summing amplifier. A sum is continuously provided at the output. A TTL pulse for each signal clocked through the shift registers is also provided at the output. This permits the use of an event counter for each valid count. In addition, an input line is provided to hold the discriminator, and hence, the sum output. This permits a given sum to be held while an A-to-D converter is sampling the output signal. The shift registers are capable of holding a sample for a maximum time of 1 msec. An appropriate source, therefore, must provide at least one count per millisecond. In addition, A-to-D conversion times are limited to 1 msec unless an additional holding is provided.

Figure 10 shows the trimpots that can be adjusted to balance the shift register input, interstage amplifier and summing amplifier. Since the dynamic range of the shift registers is limited, these trimpots should be adjusted any time a new path length range is prescribed or a new detector is used. Adjustment is done dynamically and requires some trial and error. The trimpots to the right determine the gain and offset of the analog input to shift register number one. The adjustment should be made while monitoring one of the shift registers, which are pins 3 to 18 and pins 23 to 38. The gain and offset should be adjusted such that the pulse sequence uniformly fills the full range of the shift register at a density (or path length) slightly less (10%) than the mean value expected in the measurement. This will comprise a range of +4 to +8 volts. The gain and offset of shift register number two can now be matched to shift register number one by simultaneously monitoring the output of a tap on each shift register with a dual-beam oscilloscope. For the next step in the balance it is quite useful to employ a digital voltmeter or a signal averager. The average of shift register number one should be identical to shift register number two. Minor adjustments should be made on the gain and offset of shift register number two input to satisfy this condition. If shift register number one must be trimmed, any adjustment to the gain and offset of shift register number one input also affects the gain and offset of shift register number two. The final step in the adjustment is to difference the voltage between two arbitrarily selected shift registers, one on shift register number one and the other on shift register number two. This difference should remain near zero while the density or path length is changed. Once this condition is reached, the shift registers are properly set.

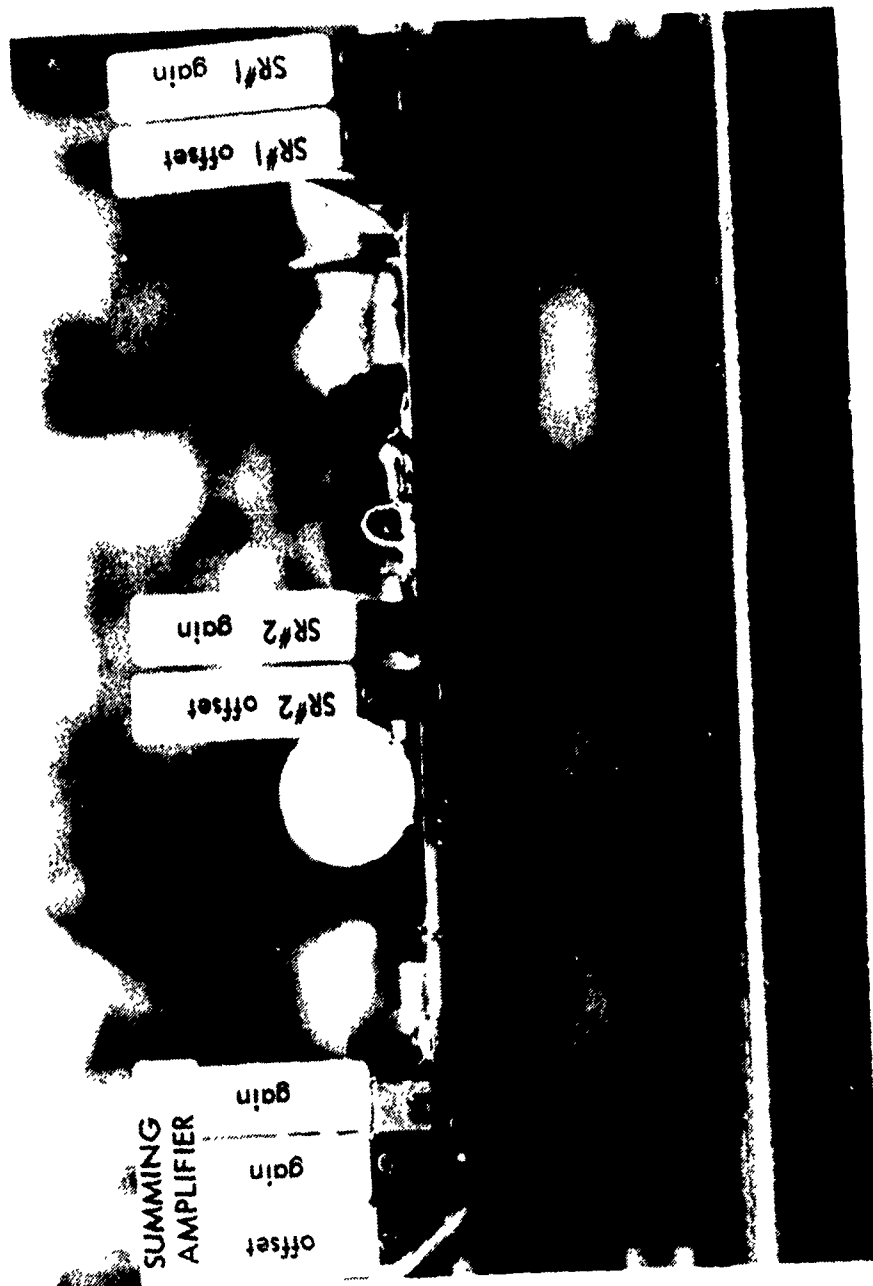


Figure 10. End view of analog PC board showing trimpot adjustments.

The final adjustment made internally is the gain and offset for the output. When this unit is used in conjunction with the current data acquisition system, the operating range is zero to 10.76. Practically, the current analog system is limited to about a 2 volt range. Adjustment is made over some positive range well away from zero, such as 4 to 6 volts.

The gain adjustment for the pulse amplifier is also made within this module. This amplifier is located in the bottom of the box. The adjustment of the final stage is made through the recessed trimpot by using a tuning wand. An ordinary screwdriver should not be used here so as to minimize the danger of shorting the amplifier. The signal should be adjusted to a value such that the largest value peaks do not exceed 1.75 volts at the lowest density expected in the experiment. This adjustment, if necessary, should be made prior to any other adjustments.

The front panel adjustments are shown in figure 11. The polarity of the bias voltage is set at either positive or negative with the slide switch, depending upon the type of detector being used. In general, a ruggedized detector requires a negative bias, while a conventional detector requires a positive bias. When in doubt, the detector's manufacturer manual should be consulted. In addition, ruggedized and regular detectors have opposite polarity signals. The signal switch should be set in the same direction as the bias for proper polarity for use by the sample and summing circuitry. A ten-turn pot provides for the proper bias setting. Seven turns corresponds to a maximum of ± 20 volts. A setting of several volts is usually adequate. The bias should be turned to zero each time the device is turned off. This reduces the risk of damage to the detector. There is also a weak dependence on signal strength with bias.

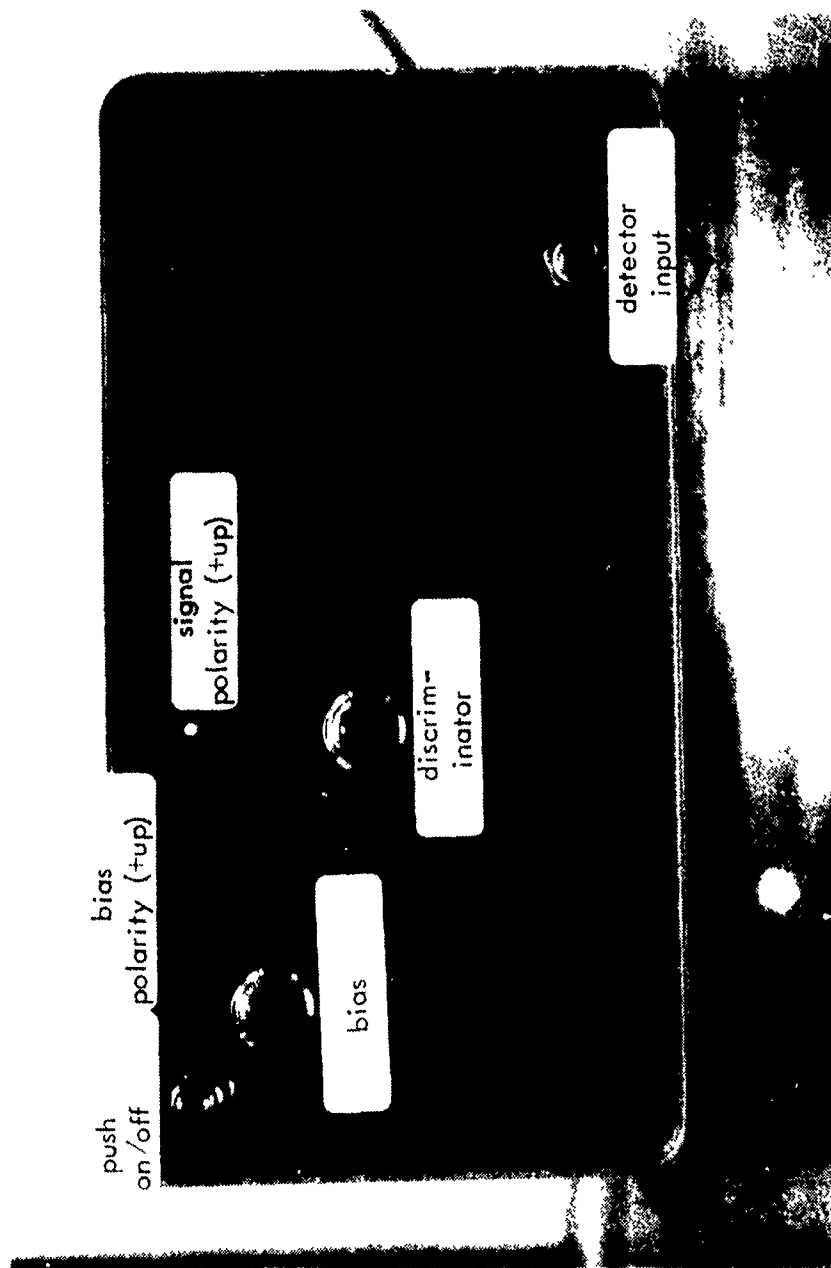


Figure 11. View of front panel of analog system chassis.

The same setting for bias should therefore be used each and every time. The other ten-turn pot adjustment on the front panel provides for the discriminator level setting. A setting from 020 to 030 was found to be adequate. The setting should be set and remain untouched throughout the course of experimentation.

The rear panel is shown in figure 12. The figure is self explanatory. Figure 13 shows the pin-out map for the output cable. This cable is compatible with the current data acquisition system.

The analog signal is currently processed by the A-to-D converter module located within the data acquisition system described in the next section. A block diagram of this circuit is shown in figure 14. The module contains the A-to-D converter and the appropriate TTL switching logic to insure proper signal transfer to memory. A Computer Labs 12-bit A-to-D converter has been provided, which has a conversion rate of 357 kHz (2.8 μ sec). Depending upon the signal delivered from the Direct Memory Access (DMA) logic, the sum is digitized when 64 pulses have shifted through the registers (event dependent) or when a prescribed time interval occurs (time dependent) independent of the number of shifts. Logic can also provide for a digitization only after both 64 pulses have shifted and a prescribed time interval is met. A hold signal is sent to the analog circuit to insure a constant value during conversion. The digitized value is then shifted into proper memory locations per DMA instructions.

The analog interface module contains eight modes of single channel data acquisition and eight modes of dual channel data acquisition possible. The data acquisition for the density probe requires the use of six modes of data acquisition. They are modes 0, 1, 2, 8, 9 and 10. Modes 0, 1 and 2 are single channel operation and modes 8, 9 and 10 are dual channel operation.

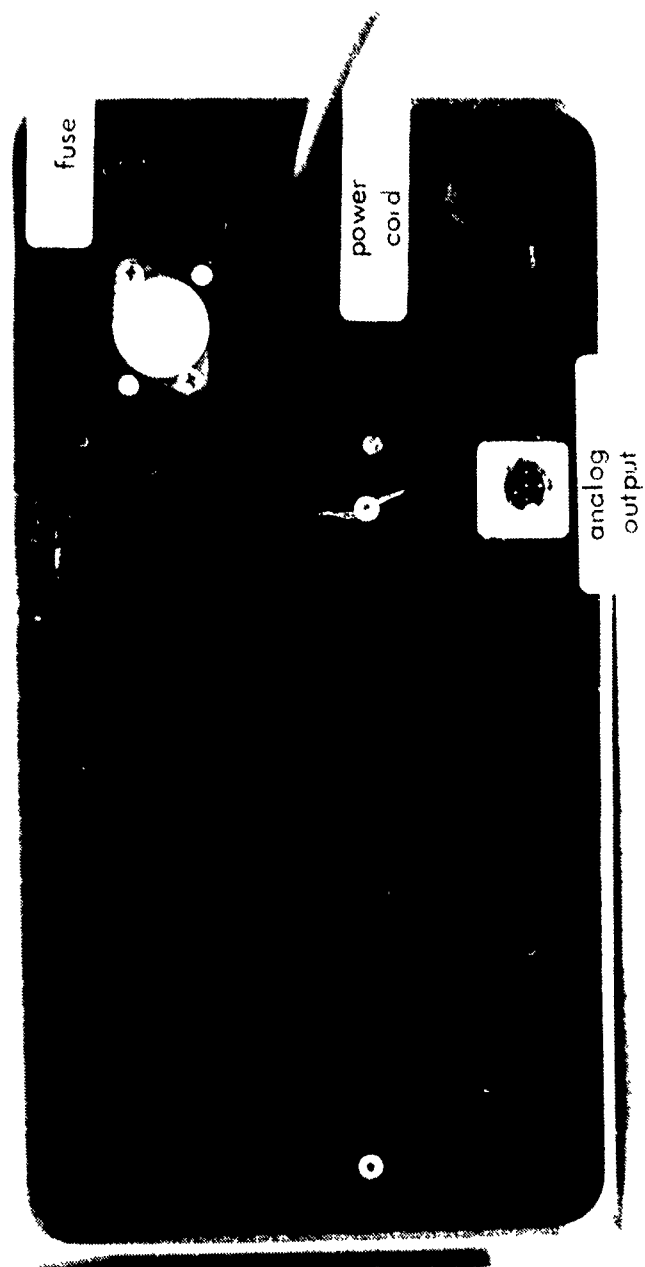
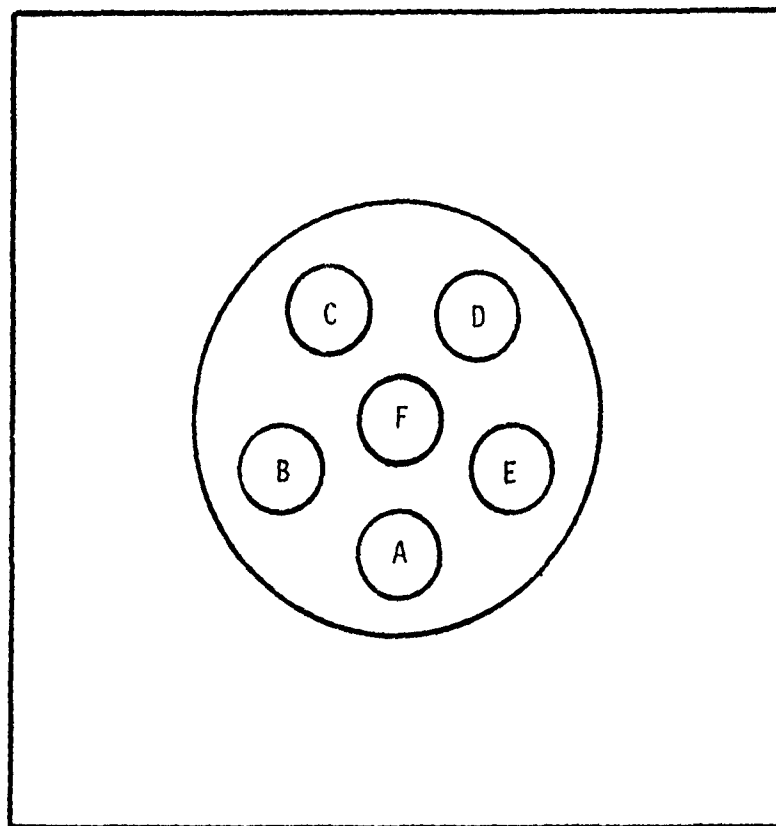


Figure 12. View of rear panel of analog system chassis.



- A - Ground
- B - Pulse Flag Output
- C - Summing Amp Output (Analog)
- D - Start of Conversion Flag (Input)
- E - N.C.
- F - N.C.

Figure 13. Pin-out map.

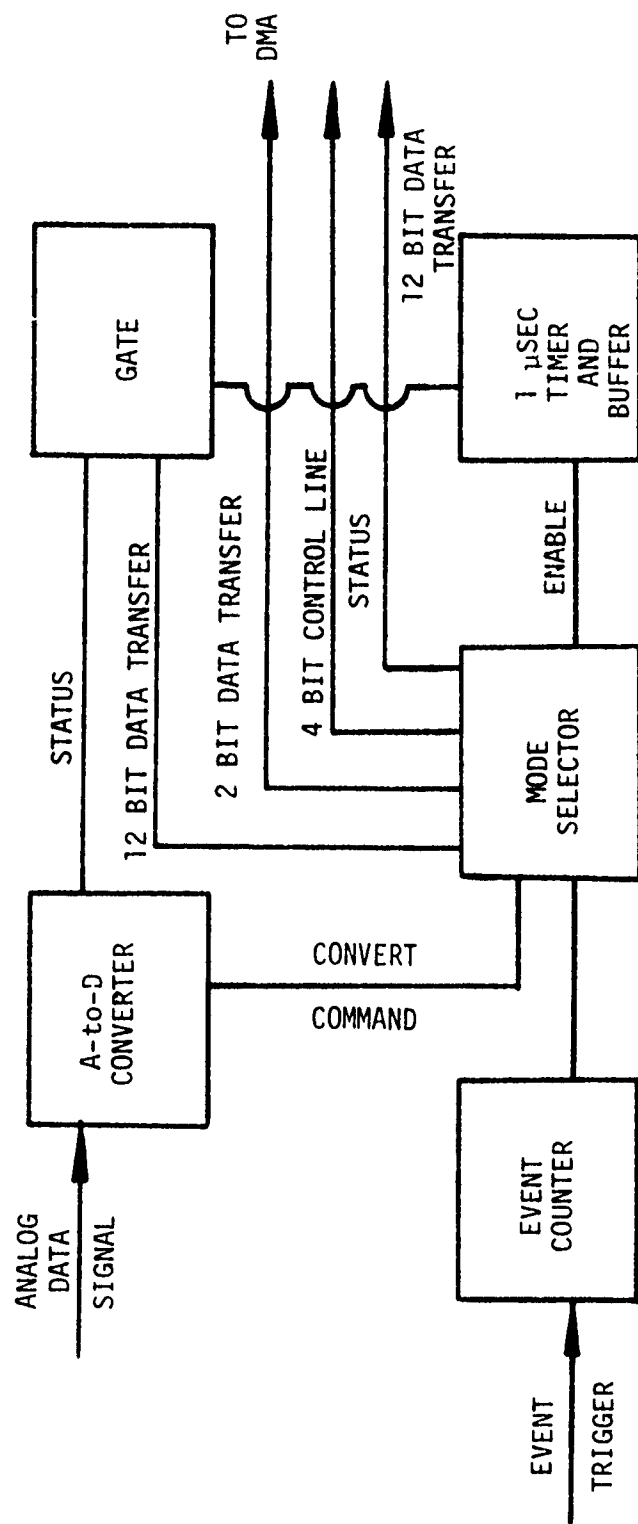


Figure 14. Block diagram of analog-to-digital converter circuitry system.

The performance of each mode is:

(1) Mode 0 - The sum of 64 counts is transferred into memory only after the shift registers are filled with 64 new counts. This is an event-dependent data transfer mode. When this mode is enabled, it continues until all 8192 words are filled.

(2) Mode 1 - The sum of 64 counts is transferred into memory only after the shift registers are filled with 64 new counts and a prescribed time interval is met. This is an event- and time-dependent data transfer mode. When this mode is enabled, it continues until all 8192 words are filled.

(3) Mode 2 - The sum of 64 counts is transferred into memory only after a prescribed time interval is met and is independent of the number of new counts which have been transferred to memory. This is a time-dependent data transfer mode. When this mode is enabled, it continues until all 8192 words are filled.

(4) Mode 8 - This mode is similar to mode 0 except that the time required to acquire 64 new counts is also recorded. When this mode is enabled, the word locations 1 to 4096 are filled with probe data and word locations 4097 to 8192 are filled with the corresponding time data.

(5) Mode 9 - This mode is similar to mode 1 except that when it is enabled, 4096 words are filled with data and the remaining words are filled with zeros.

(6) Mode 10 - This mode is similar to mode 2 except that when it is enabled, 4096 words are filled with data and the remaining words are filled with zeros.

These various modes are accessed through the software package.

The system as described herein provides for the analog sum and the proper digital conversion. It is important to note that the analog output

can be displayed or processed by any conventional method, just as one would process any other low impedance analog signal. The A-to-D converter and the digital system described in the next section can also be used for other signal processing and is a stand alone unit.

V. DIGITAL DATA ACQUISITION SYSTEM

The digital data acquisition system is a dedicated microprocessor computer. The central processor is a Texas Instruments 9900 16-bit microprocessor. It has dedicated components for active memory and acquisition of data. With the memory allocation as it currently exists, its function is limited to the acquisition and processing of data directly resulting from the density probe analog system described in Section IV.

The system contains the following modules: Central processor unit (CPU), read only memory (ROM) board, three random access memory (RAM) boards, direct memory access (DMA), tape deck, front panel display (FPD) and the A-to-D converter board. There are also, of course, the associated power supplies for these units. These units communicate with each other via a common bus. These units, as well as assembly of the system, were provided by Real Time Design, Inc.

The CPU contains the 9900 microprocessor as well as the various driver circuits for communicating with the other units. The ROM board contains nonvolatile memory which is filled with the assembled software package that drives the microprocessor. The total memory on this board is 4096 16-bit words, and the required code nearly fills this entire memory. It contains the operating system as well as the necessary code for the analysis of the density probe data. The discussion of the operating system is discussed later in this section and the density probe data reduction software is discussed in the next section. The three RAM boards

contain 12,288 words of volatile memory; 8192 words of memory are reserved for the density probe data. The software treats these data as two sets of 4096 words.

The basic memory cycle of the data acquisition system is 330 nsec with each operation requiring 2 to 58 cycles to complete. The majority of the instructions require 4 to 8 cycles.

The DMA permits the random access memory to be filled directly with data from the A-to-D converter board without commands from the CPU. The primary advantage of this is that memory may be filled much more rapidly. DMA transfers require a minimum of 660 nsec to acquire control and transfer the first byte or word. Each additional transfer requires a minimum of 330 nsec. If memory is released between each transfer, the worst case transfer time is 1.2 μ sec per transfer. A secondary advantage, although not used in this case, is that the CPU can be executing while the DMA is filling memory. The current DMA configuration permits the acquisition of two channels of data in an alternate manner and subsequent loading into separate memory blocks.

The CPU module features the TMS 9900 microprocessor. Implemented on the module (although not necessarily supported by firmware) are 16 levels of priority interrupt and a crystal controlled asynchronous receive/transmit device with eight program selectable input/output channels. One (CH. 7) is committed to the RS232C interface included on the module; one (CH. 6) is committed to a 20 mA teletype compatible current loop with tape reader control; one (CH. 0) TTL level channel is committed to the tape unit. There are five uncommitted channels (CH. 1-5). Rate, mode and format are software controlled by a TMS 9902 UART device.

Other features include two user programmable real time clocks, 16 bits

of input/output committed to front panel and tape control, 22 uncommitted bits of input/output, and a hardware single step circuit for manual program intervention and test.

The ROM module supports up to 16K bytes of 2708 EPROM read only memory. The board must be installed on a 16K address boundary (0000, >4000, >8000, or >C000) with only the portion filled being addressed.

The RAM modules (three) consist of 8K bytes each of static random access memory (type 21L02) and are installed on even 2K increment addresses (0, >2000, >4000, >6000, >A000, >C000, >E000). Provision is made for a one cycle wait state if memory cycle time falls below 450 nsec. The modules require byte level addresses, but may be configured, as in this particular use, as 16-bit wide memory. This yields 4096 16-bit words per module.

The DMA module has several options available. Only those applicable to this particular installation will be covered. Circuitry is provided on the module for two bidirectional DMA channels using 16-bit wide data paths. Mode of operation, direction of transfer, location and length of the transfer and end action responses are all available to the programs.

Power is derived from four separate modules. Available power is:

- + 5 Vdc at 12 A
- 5 Vdc at 3 A
- +12 Vdc at 1.5 A
- 12 Vdc at 1.5 A

Nominal power consumption is 100 watts. The system is protected by a 1.5 A slow blow force at the rear of the cabinet. A toggle switch on the front panel controls power on/off. Input power is 110/220 Vac at 50-80 Hz. The unit is supplied connected for 110 volt operation. A 220 volt operation requires

internal connection changes at the power supplies.

Plug the main power cord into a 110 Vac 3 wire outlet with integral ground. Do not operate the unit ungrounded.

WARNING: Severe electrical shock may result from contact with the metal computer case if this unit is operated without a functional earth ground to the power cord ground lead.

The unit may be operated with the cover removed if required, but this operation exposes the equipment to potential damage from foreign objects and is not recommended.

Connect any standard terminal with an interface meeting EIA RS232C specifications to the DB25 socket on the rear of the cabinet. Turn the terminal on, then turn on the computer with the switch on the front panel. Press the "RESET" button above the power switch and enter the letter "A" on the terminal. Firmware is provided to determine which of the available transfer rates (110, 300, or 1200 baud) is being used. When the terminal responds, proceed as outlined in Sections V and VI.

CAUTION: Always remove tapes from the tape deck before turning power off or on to prevent damage to tapes or loss of data.

The FPD is shown in figure 15. This display is principally provided to display the mean density in the upper display and the present standard deviation divided by the mean in the lower display. Secondly, it provides other messages: An F is displayed when it is turned on; a D is displayed when the density probe data reduction routine commences; and E, as shown in the figure, is displayed during data acquisition; a C is displayed when data acquisition is complete; numerical displays are displayed as fixed point numbers and the location of the decimal point is as shown. The upper panel permits the display of a positive number no greater than 9.999, and the lower panel permits the display of a positive number no greater than 99.9. When a number is negative or greater than these values, a dash is displayed in each location.

Also shown in figure 15 is the location of the cassette tape unit. The software provides for data to be transferred serially to and/or from the tape unit. Shown at lower right is the on/off switch and the reset button. The reset button automatically resets the software back to the starting point in the operating system.

The rear panel is shown in figure 16. Access for 15 bus lines are shown. Only one, however, is used. The top one in the third column is an RS232C plug and provides for direct communication with standard terminals. The plug on the lower right provides the cable connection between the analog system and the A-to-D converter board. In the lower left are the fuse, plug and the power cord. A 110 volt dual outlet is also provided. This outlet is in series with the front panel switch. Common equipment such as the analog system and the terminal can be turned on or off by the single switch. Shown also are the exhaust fans which provide the proper cooling for the system.

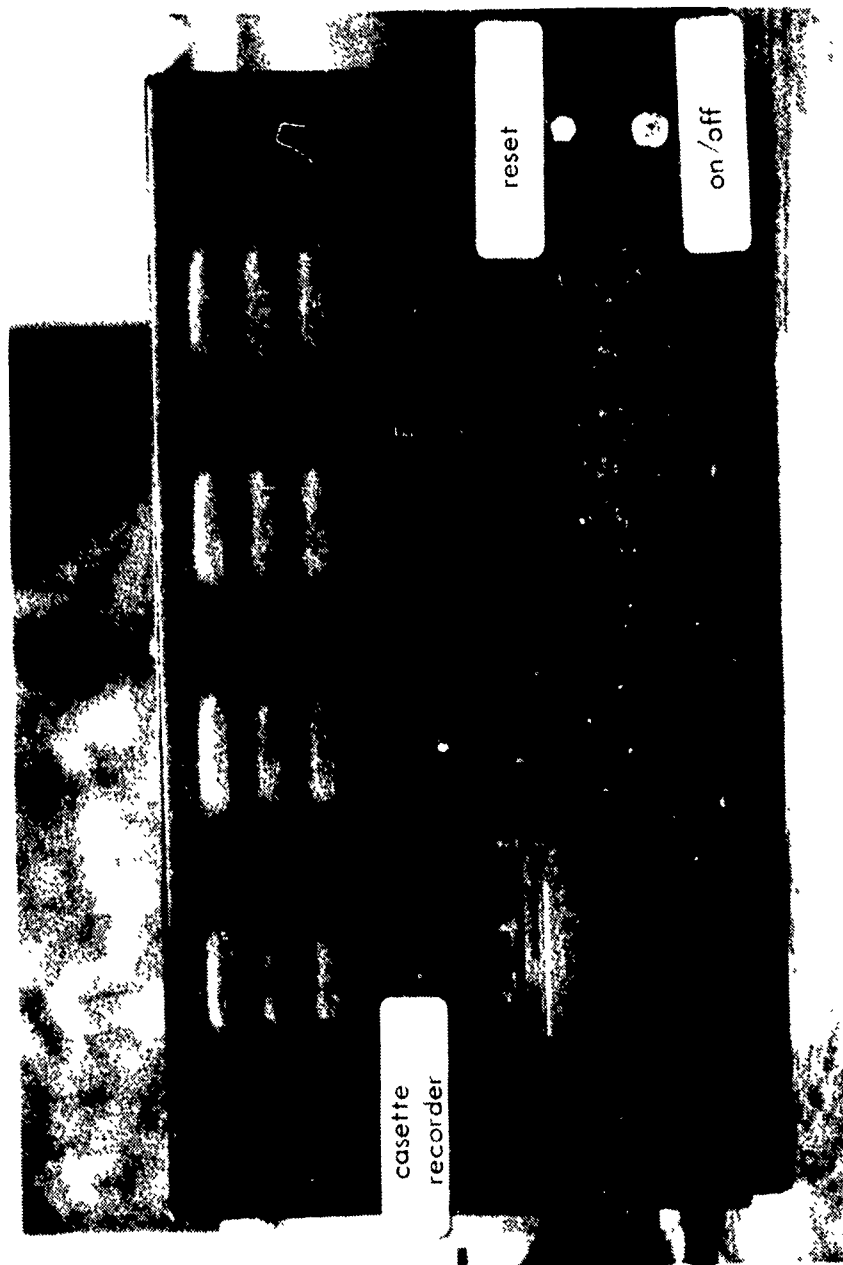


Figure 15. View of front panel of data acquisition system.

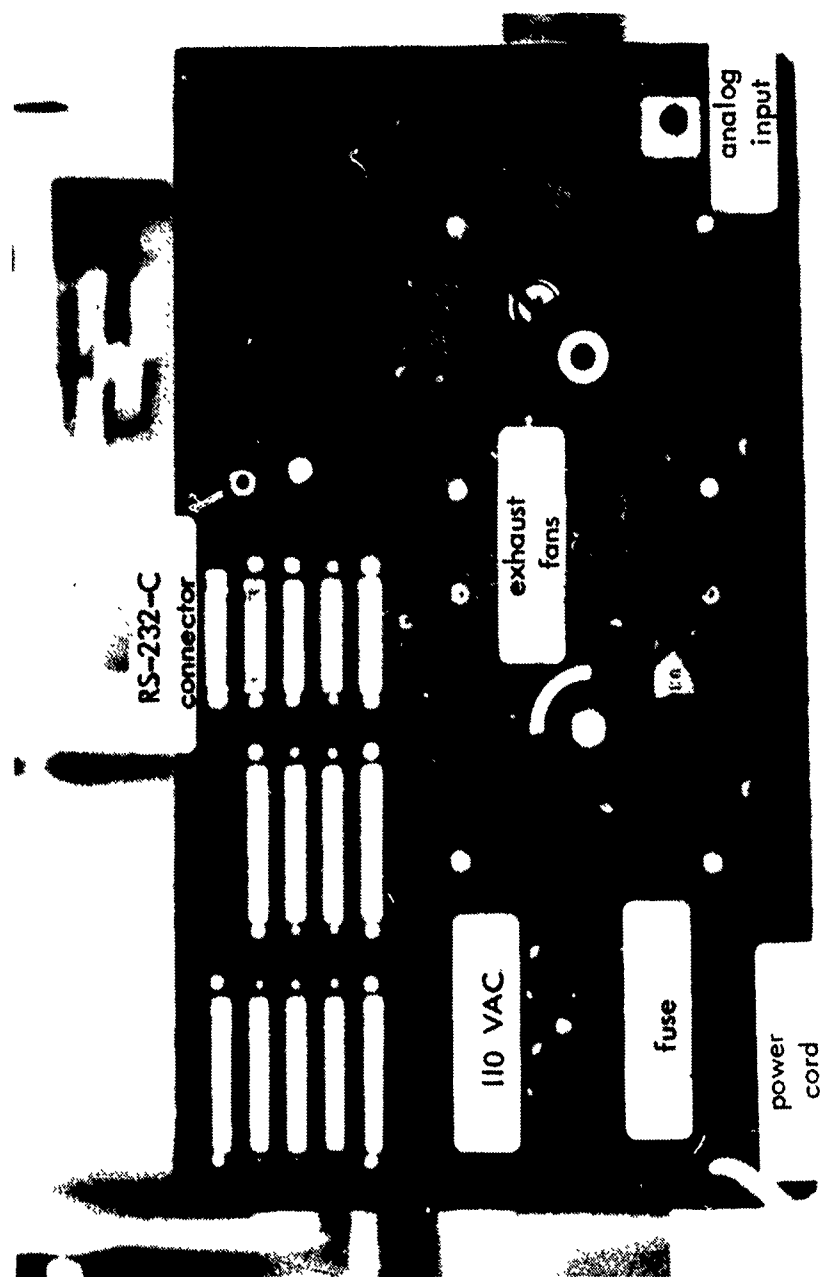


Figure 16. Rear view of chassis of data acquisition system.

The RTD 99 microcomputer provided with the density measuring system contains a small self-supporting executive module which is useful for maintenance and minor program modification. The supported commands are described below. The syntax required is shown underlined and in capital letters. Each entry is terminated by a "RETURN" character. All entries are in hexadecimal. Lower case parts of the command may be omitted.

1. COMpare AAAA,BBBB,CCCC

Compare the contents of memory in a block beginning at AAAA and ending at BBBB with a block beginning at CCCC. If the source address from block AAAA-BBBB does not compare with the memory in the same relative position in the block starting at CCCC, the address failing to compare, the contents of that address, and the contents of the compared data are displayed.

COM 2000,2002,3000

2000 = 1234 3000 = 1233

DISPLAYED:

2000 - 1234 1233

2. DISplay AAAA,BBBB

Display memory from hexadecimal location AAAA through BBBB.

3. FILL AAAA,BBBB,CCCC

Fill memory from locations AAAA through BBBB with data CCCC.

4. GOTO XXXX

This command causes the computer to execute the assembled code at

the location in memory XXXX and it continues to execute subsequent commands in memory until it reaches the stop command or the reset button is pushed.

5. LEAd

Rewind the tape and erase from the start of the tape until a character is entered from the keyboard, then stop the tape.

6. LOAd

LOAd AAAA

Load the data on the next tape segment at the address specified on the leader. If AAAA is specified, add that value to the address on the tape. If AAAA is not entered, assume 0.

7. MOVe AAAA,BBBB,CCCC

Move the contents of a block of memory beginning with location AAAA and ending with location BBBB to a block of memory starting with address CCCC.

8. REWind

Rewind the tape.

9. RUN

Commence execution of data acquisition and analysis program as described in Section VI.

10. SAVe AAAA,BBBB

Write memory contents beginning with AAAA and ending with BBBB to

tape. A one-second blank leader is written followed by a leader consisting of the following hexadecimal data:

F0 F2 AAAA BBBB F1 DATA

and ending with the binary character F1

11. STOp

Stop the tape where it is.

12. SUBstitute AAAA

Display the contents of memory address AAAA and permit alteration of that data. If any value 0-9 or A-F is entered, the value is entered. If "RETURN" is entered, the operation is terminated. If a space is entered, the data is unchanged and the next location is displayed.

EXAMPLE:

Memory Contains

ADDRESS	0	2	4	6	8	A	C	E	10	12	14
	0000	0002	0004	0006	0008	000A	000C	000E	0010	0012	0014

SUB 0000

0000 - 0000 0002 0004 1234 0006 RETURN

NEW MEMORY

0	2	4	6	8	A
0000	0002	1234	0006	NO CHANGE	_____

VI. DESCRIPTION OF SOFTWARE USED IN DENSITY PROBE DATA REDUCTION

In addition to the software described in Section V, there is an extensive software package which has been assembled to analyze the data generated by the density probe analog system. This software has been written in assembly language. This permits not only increases in the speed of the analysis and saves memory space, but also permits direct interfacing with the communications register unit. This code, when assembled, uses about 6K words of read only memory. A flow chart of the code is shown in figure 17.

When the computer displays an exclamation point (!) on the terminal, the operator merely enters RUN and a carriage return to execute the software package. Simultaneously, the front panel display changes the F display to a D. The computer then returns with the following message:

```
DENSITY PROBE DATA ANALYSIS  
READ DATA FROM TAPE (Y OR N)?
```

At this point a Y is entered if previously stored data are to be used and an N is entered when new data are to be acquired. The tape routines shall be explained later in the section. Messages ending in a question mark require a Y or N. No carriage return is required. If a character other than a Y or an N is typed, the message is repeated.

When an N is entered, a series of messages occur, each of which require data entries. The first message is:

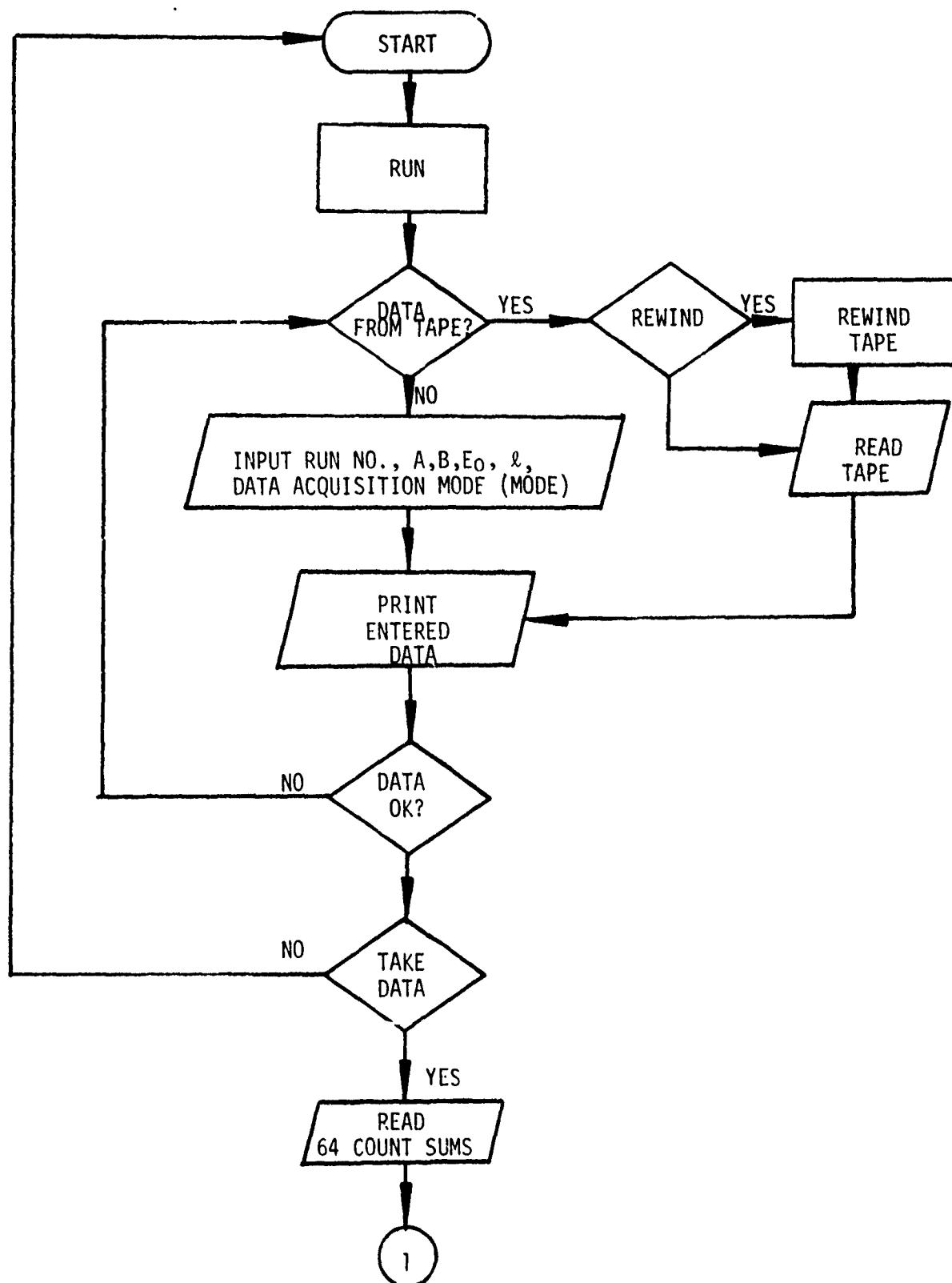


Figure 17. Flow chart of density probe data reduction program.

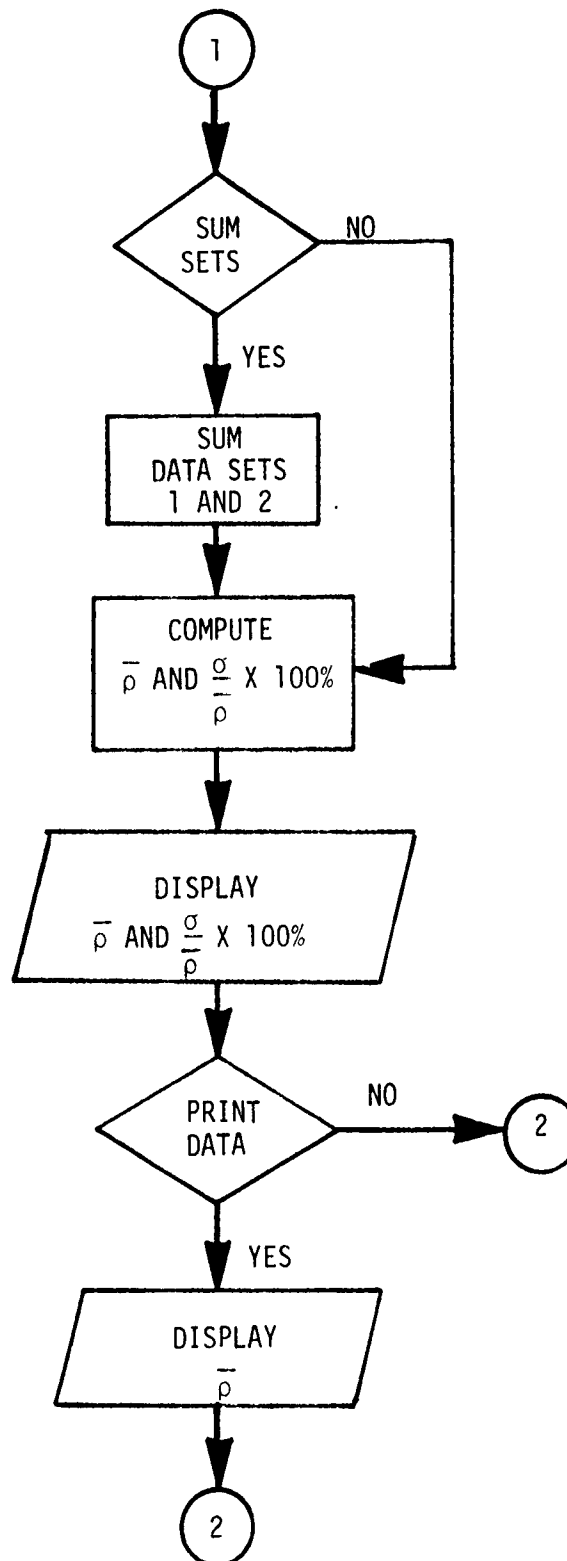


Figure 17. Continued.

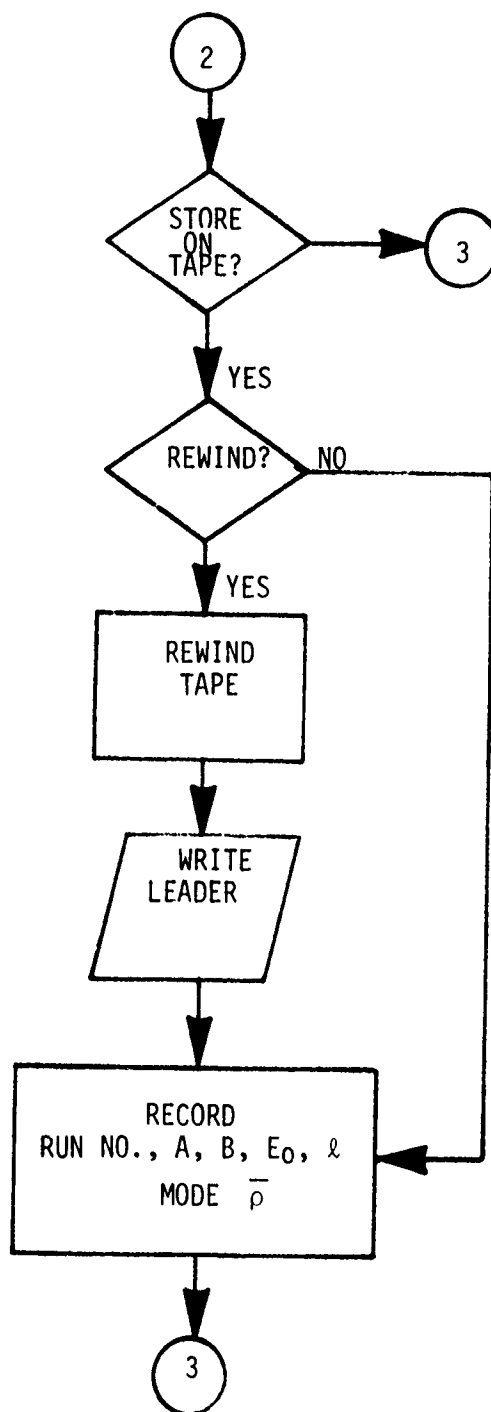


Figure 17. Continued.

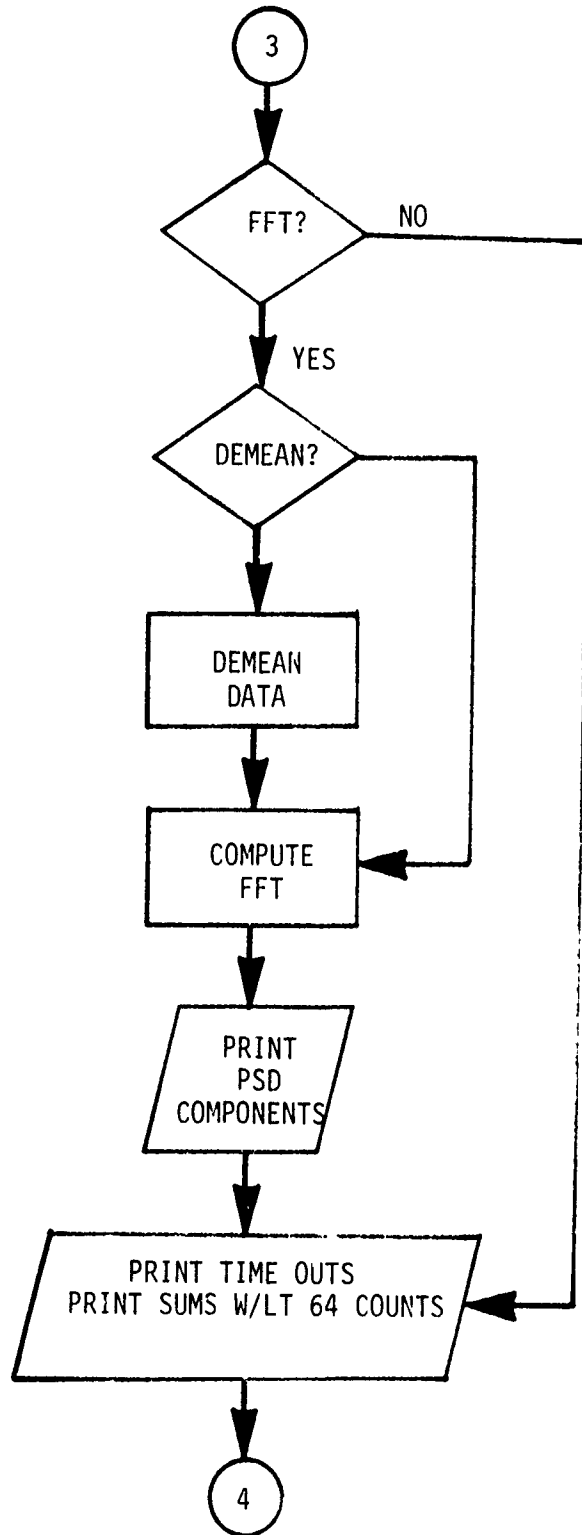


Figure 17. Continued.

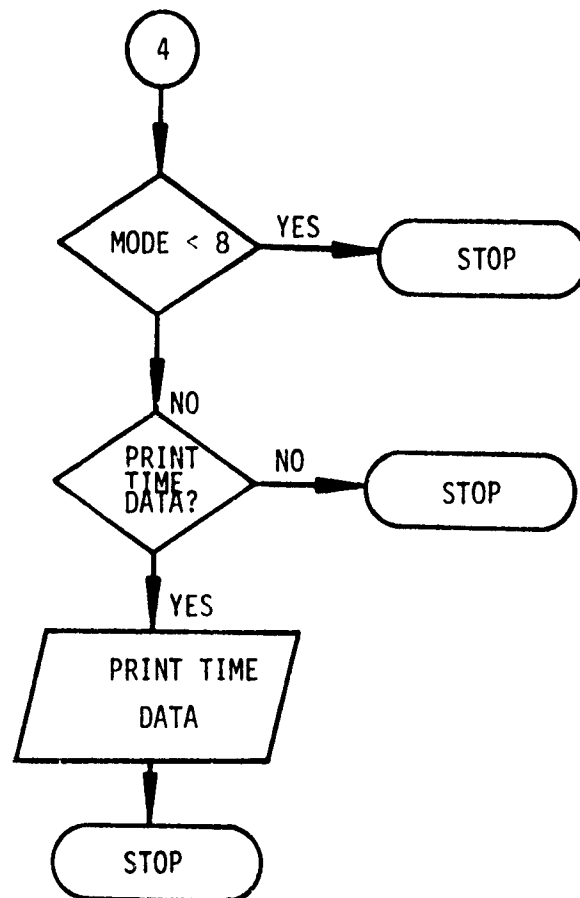


Figure 17. Continued.

ENTER RUN NO.

This provides the necessary identification of the data. The next six messages relate directly to constants germane to a particular run. They are:

ENTER A

ENTER B

ENTER EO

ENTER PATH LENGTH (CM)

ENTER TIME WINDOW (MICROSEC)

ENTER DATA ACQUISITION MODE

A, B and EO are the calibration constants of equation (6) in Section II of this report. If the new data to be acquired is a calibration run, then by using an A=1, B=1, and EO=0 the value of E itself will be processed. Entry of all the above data must always be a fixed point number. The number is also restricted to four decimal numbers to the right of the decimal point. If entry of a fifth number is attempted, the program automatically truncates and enters the number. If an error is made, such as entry of a second decimal point, a letter, a comma, etc., the program automatically re-enters the previous message. After the operator has entered the number, he must enter a carriage return to send the number to the computer. The entry of all numbers occurs in this fashion.

Besides entry of the calibration constants, the path length must also be entered. Since a calibration depends upon the path length as described in Section II, path lengths other than the one used for calibration may be used when desired. As noted in the message, the proper dimension is centimeters. When a calibration run is being made, a value of one is used here

and the path length is recorded separately. The time window is relevant for modes 1, 2, 9 and 10. This prescribes the time in microseconds at which an analog sum will be converted to digital form and entered as data. When modes 0 or 8 are run, this number is irrelevant and any number may be entered. The data acquisition modes are summarized in Section V. The desired number is entered here and is the last data entry.

After these data are entered, the computer returns with the summary of entered data and the number of data sets. When modes 0, 1 or 2 are used, there will be two sets of data which contain density probe information. When modes 8, 9 or 10 are used, there is one set of density probe data the second set contains the time information as described in the previous section.

In addition to the display of data, the following message is presented:

DATA PROPERLY ENTERED?

When the response is N, the program returns to the start of the data entry message. Any incorrect entry can then be corrected. If an entry was correct, the operator merely enters a carriage return to skip to the next entry. With a response of Y to the question above, the program first sets up the DMA software and then returns with another question:

TAKE DATA?

A response of N causes the computer to exit the program and return with an exclamation point (!). With a response of Y the computer executes a carriage return and then immediately begins recording measurements. At this time, an E is displayed on the front panel. When data taking is complete, it executes a line feed and displays a C on the front panel. The following question is then displayed:

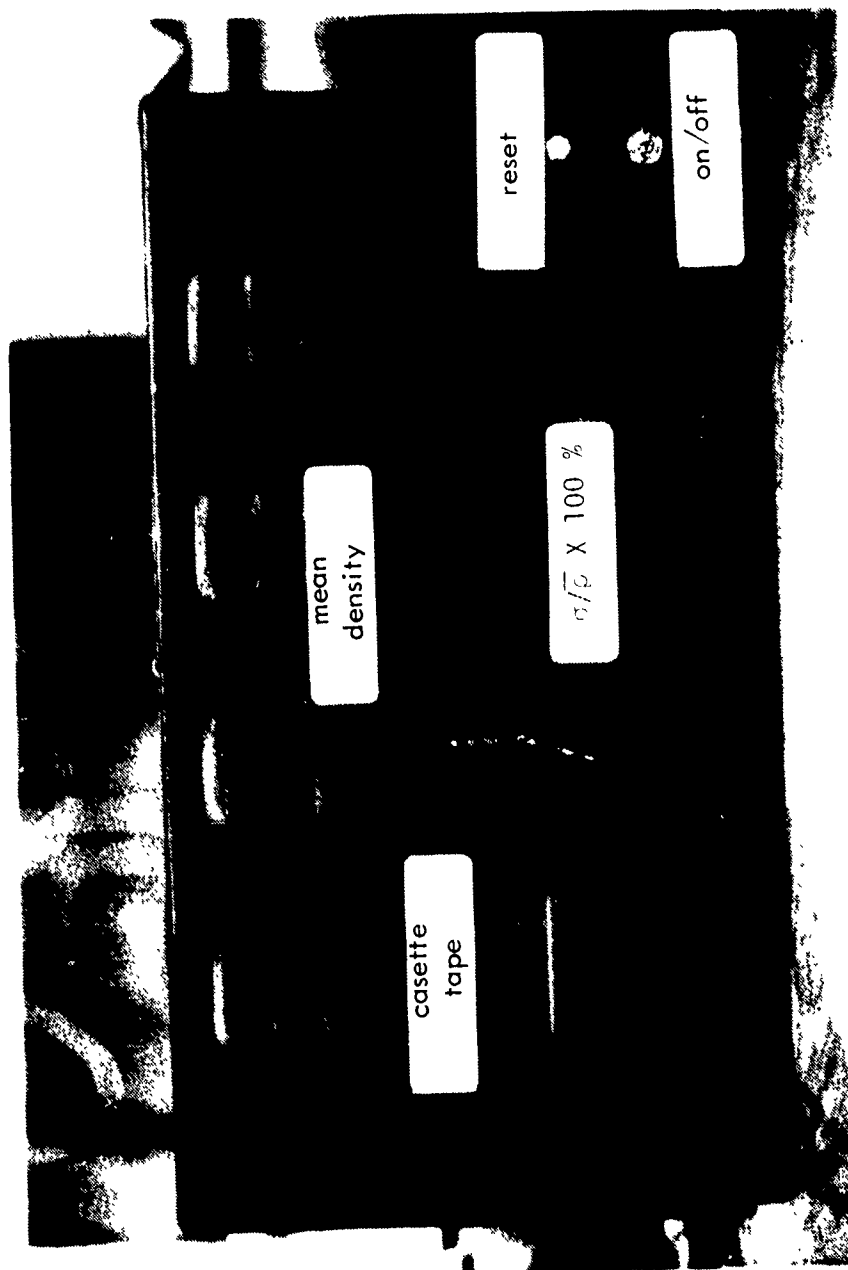


Figure 18. View of front panel of data acquisition system showing display of mean density and percent fluctuations.

SUM SETS?

A response of Y to this query causes the two sets of data to be combined into one set by summing adjacent 64 count sums. The first set contains sets with 128 count sums while the second set contains the original 64 count sum. It is meaningless to sum sets when time data has been recorded (Mode 8, 9 or 10).

The next message is:

PRINT DATA?

A response of Y results in the serial display of the data reduced to density values in units of mg/cm^3 . This output can be terminated at any time by the entry of an X from the keyboard.

The next message is:

STORE ON TAPE?

A response of Y permits storage on tape.

The next message is:

REWIND?

A response of Y causes the tape to rewind.

Upon completion of the rewind the tape automatically starts forward at a normal speed and begins putting a leader on the tape. Simultaneously, the next message is displayed:

STOP LEADER?

After about ten to fifteen seconds of leader generation, an entry of any key from the keyboard will result in cessation of the leader and begin immediately the recording of the data.

Once the data have been recorded, the proper spacer will be entered so that the next record is ready to be recorded. Six to seven data records can be recorded on each side of a typical cassette tape. When data are read from the tape, the rewind option is available but there is no stop leader command. Whether a tape is being read from or written to, the data are blocked in a serial fashion; therefore, a tape should not be removed when additional data sets are to be read or written.

The next message after the tape is recorded is:

FFT?

A positive response permits a fast Fourier transform (FFT) of the data.

The next message is:

DEMEAN?

A positive response to this message subtracts the average of the particular data set of 4096 points. The FFT is taken in groups of 512 points. The 257 relative power spectra values are displayed sequentially. The purpose of the demean is to reduce the effect of the expected large DC component. It usually is not zero however, since the mean of the 4096 points is not necessarily the mean of the particular set of 512 points. The output from the FFT can be terminated by the entry of an X from the keyboard.

The next two messages indicate the number of points with time-outs and the number of points with less than 64 counts. Both refer to the occurrence of less than 64 new counts in any one time interval. This output is meaningful only for modes 1 and 9.

When mode 8 is used, the second set of data is the time required to obtain 64 counts. The final message of this set of software permits the

display of this time data. It is:

PRINT TIME DATA?

Again, this display may be ended prior to a complete display by the entry of an X from the keyboard.

VII. CALIBRATION

The inverse relationship between density and path length as shown in equation (2) suggests two equivalent means of calibration for the probe. One technique would be to use a sealed pressure vessel and vary the density by controlling the pressure in this vessel. The other technique is to vary the path length while holding the density constant. The advantage to the path length variation technique is that it can be accomplished virtually anywhere provided the mean density is known. It does, however, require a probe such as the one described in Section III. Both techniques were used in the calibration of the probe.

There are subtle differences in the two techniques of calibration. Varying the path length also causes the view factor to change, and hence, the count rate. This is not a problem, as long as several criteria are satisfied. First of all, the detector must not be moved too far from the detector to cause the count rates to become so infrequent that the shift registers fail to hold a signal properly. As discussed in Section IV, this requires a minimum of a count every millisecond. Secondly, several difficulties are encountered if the detector is moved too close. First of all, the preamplifier and/or the shift registers can become saturated. This, of course, will be obvious in the calibration. Another problem is the change in the view factor which can be especially critical if the diameter of the source and/or detector becomes an appreciable fraction of the path length.

When this occurs the variation in the path length affects the distribution of residual energy, thus reducing the precision in the measurement. For a 2 mm diameter detector and source and a 1 cm path length, the path length variation is 3.7%. At short path lengths, backscatter also becomes a problem. This occurs when alpha particles emitted toward the substrate in a direction opposite to the detector are reflected back. After passing through the polonium they possess considerably less energy than those which are emitted directly forward. For ranges of less than 0.5 mg/cm² these back-scattered particles have been observed and found to affect the measurement. Beyond this range the energies drop to values that are on the order of the noise level.

Measurements with a fixed path length were accomplished at Precision Measurement Equipment Laboratory (PMEL) at the Air Force Weapons Laboratory. The probe was placed in a sealed pressure vessel which is capable of withstanding a pressure variation of ± 1 atm. This vessel was connected to a balance valve which controls the pressure by balancing the leak rates from a compressed air supply and a vacuum system. It was found that the pressure could be controlled to within 0.1 torr. Temperature within the vessel was measured with a standard mercury thermometer. During any one test, however, it was observed that the temperature changed no more than 0.2°C.

Three calibration runs were recorded with this pressure vessel arrangement. All tests were similar. Table 2 gives the results of the first calibration run. The data acquisition mode for cases #1 and #2 was mode 0, and thus 4096 sums of 64 counts were recorded for each set. Case #3 was recorded in mode 2 operation with a sample every millisecond, averaging about 40 new

Table 2. Data from case #1 tests. (Discriminator - 0.30;
bias - 2.00; path length - 1.95 cm)

P(Torr)	T(°C)	V	V	V	V	V	V	V	$\sigma_P \times 100\%$
610	25.1	2.74	2.74	2.75	2.76	2.74	2.76	2.76	3.5
600	25.1	2.81	2.81	2.80	2.79	2.89	2.82	2.82	3.6
590	25.2	2.87	2.86	2.87	2.87	2.87	2.88	2.88	3.5
580	25.2	2.92	2.91	2.92	2.92	2.92	2.92	2.92	3.3
570	25.3	2.96	2.97	2.96	2.95	2.96	2.96	2.96	3.1
560	25.3	2.99	3.00	2.99	2.99	2.99	3.00	3.00	2.8
640	25.4	2.64	2.64	2.64	2.63	2.63	2.63	2.63	3.7
650	25.4	2.57	2.58	2.57	2.57	2.58	2.57	2.57	3.7
660	25.4	2.52	2.52	2.52	2.51	2.51	2.51	2.51	3.6

counts with each run. This run and several other trial runs indicated that there was virtually no difference between mode 2 and mode 0 operation.

The last column of Table 2 indicates the average value of the standard deviation divided by the mean. Note that this value decreases at the high and low pressure limits. At these limits the shift registers are not operating over a full range. Data are therefore "clipped" at the ends of the scale, and hence the decrease. Figure 19 is a graph of the mean values as a function of density. Figure 20 is a graph of range versus mean values. Also shown on figure 20 is the least squares result for the range shown. A linear fit was chosen because it is not possible to determine the vacuum condition (E_0 value) due to the limited dynamic range. A linear fit has proven to be adequate.

Of interest is the precision at which the density can be measured. The logarithmic derivative of the equation in figure 20 will provide a relative measure of this precision. Repeating the least squares fit here

$$\rho l = 0.443 (7.41 - V) \quad (21)$$

The logarithmic derivative is

$$\frac{d\rho}{\rho} = \frac{V}{7.41 - V} \frac{dV}{V} \quad (22)$$

$$\text{at } V = 2.64 \quad \frac{d\rho}{\rho} = 0.553 \frac{dV}{V} \quad (23)$$

$$\text{for } \frac{dV}{V} = 3.7\% \quad \frac{d\rho}{\rho} = 2.0\% \quad (24)$$

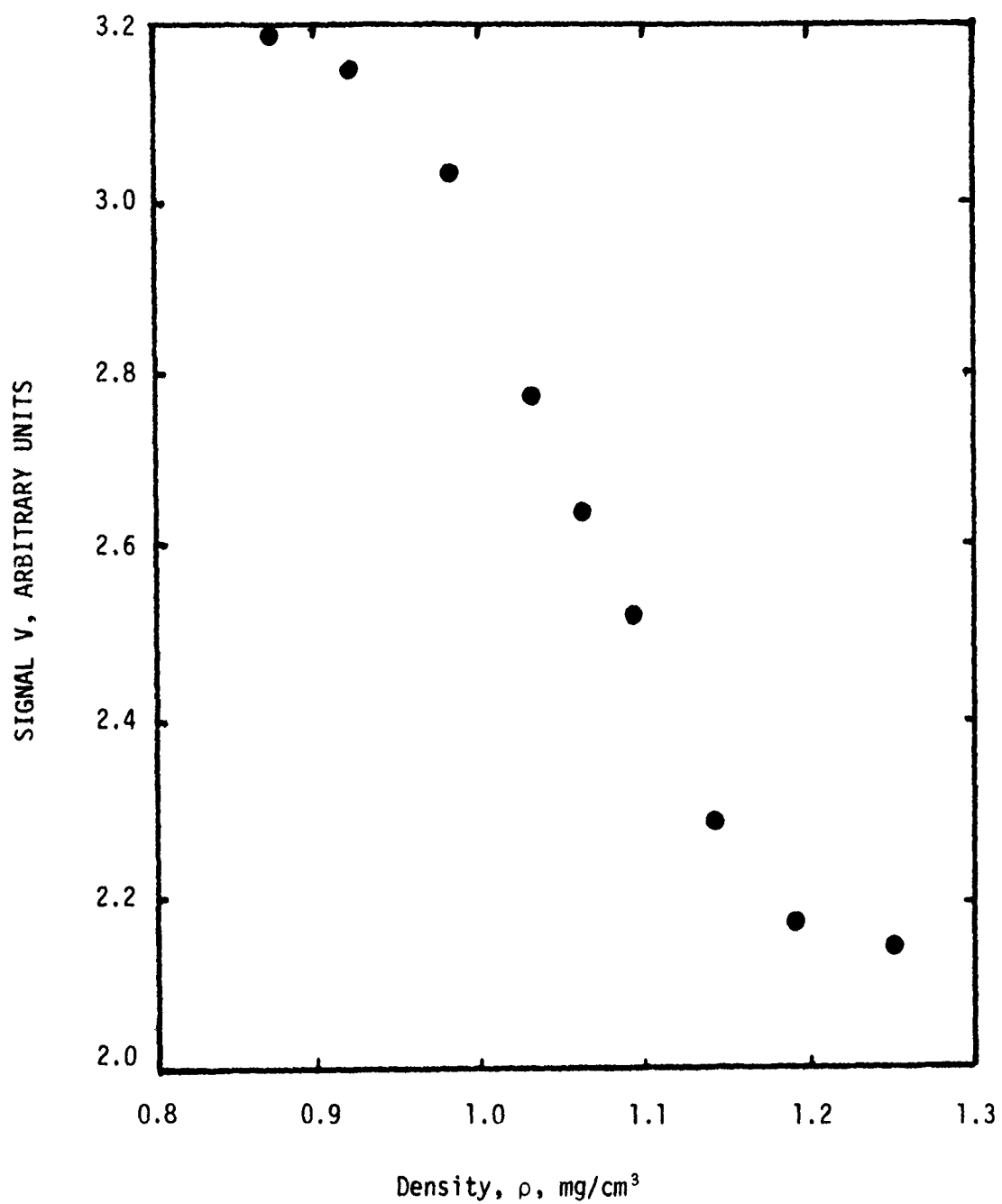


Figure 19. Density versus signal for case #1 calibration.

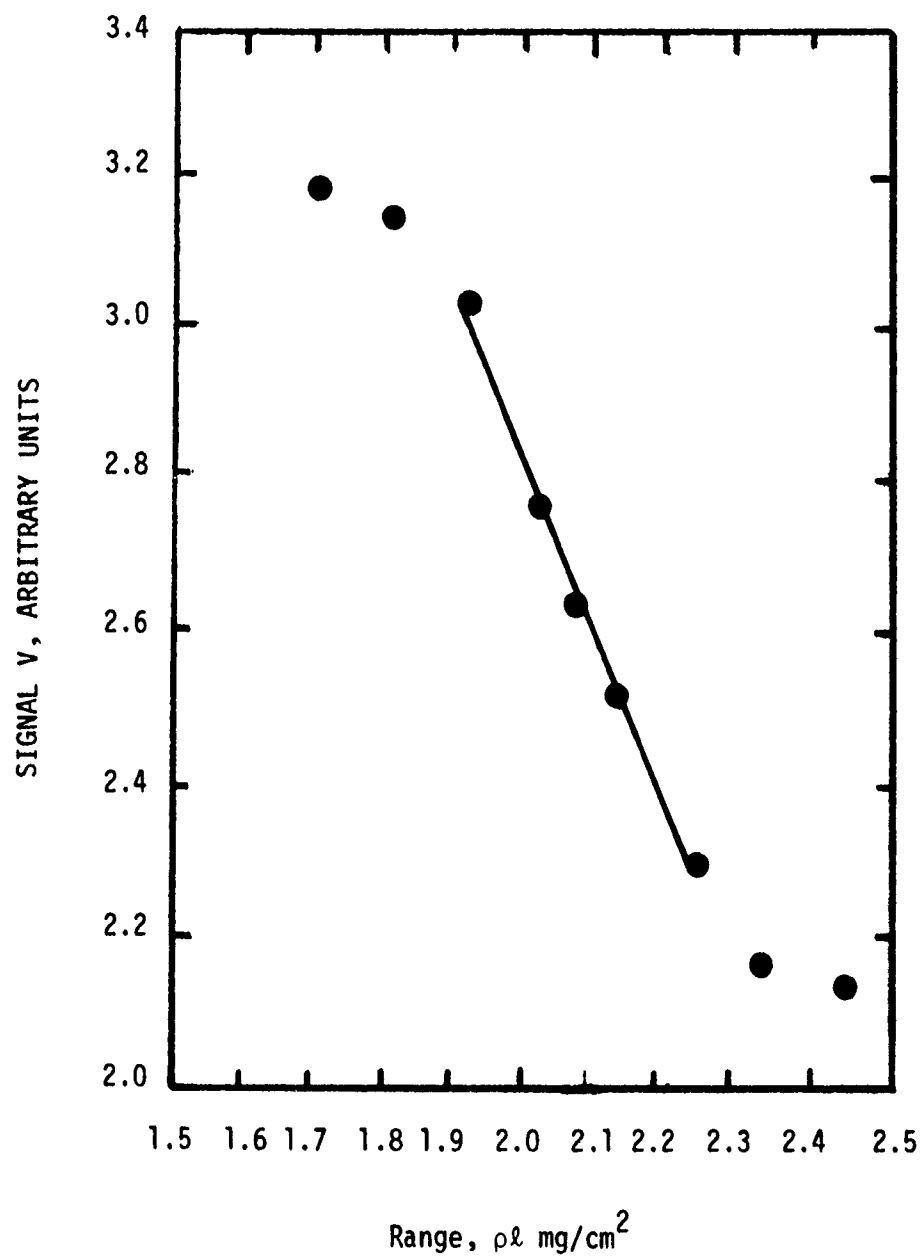


Figure 20. Range versus signal for the case #1 calibration.

Based upon this calibration one could expect a 2% precision in the density measurement.

Figure 21 is a graph of the results of case #3 where mode 2 was used to collect the data. Here more data were taken over the linear range. The results are essentially the same as presented in figure 20. The difference in the ordinate values is due to the higher bias setting on the detector. The bias was found to have a slight effect on the output. Experience has demonstrated, however, that there appears to be no particular advantage of one bias setting over another as long as the setting is above zero and is fixed for a given calibration.

In addition to basic calibration tests, the effect of discriminator settings was also examined. The results are shown in figure 22. The purpose of the discriminator is to eliminate the noise and low level counts. As the level is raised more and more, low level counts are eliminated. As expected, the standard deviation decreases as the discriminator level increases. It was expected that the signal would increase as the discriminator setting was increased. This apparent anomalous behavior is not understood at this time.

As a result of the tests at PMEL, several recommendations can be made with regard to the operation of the density probe system.

1. A discriminator setting as low as possible appears to yield the best results. A setting of 0.30 appears to be adequate for all conditions.
2. The signal level increases with increased bias. The bias should be fixed during calibration and held at that value throughout testing in order for it to be valid.

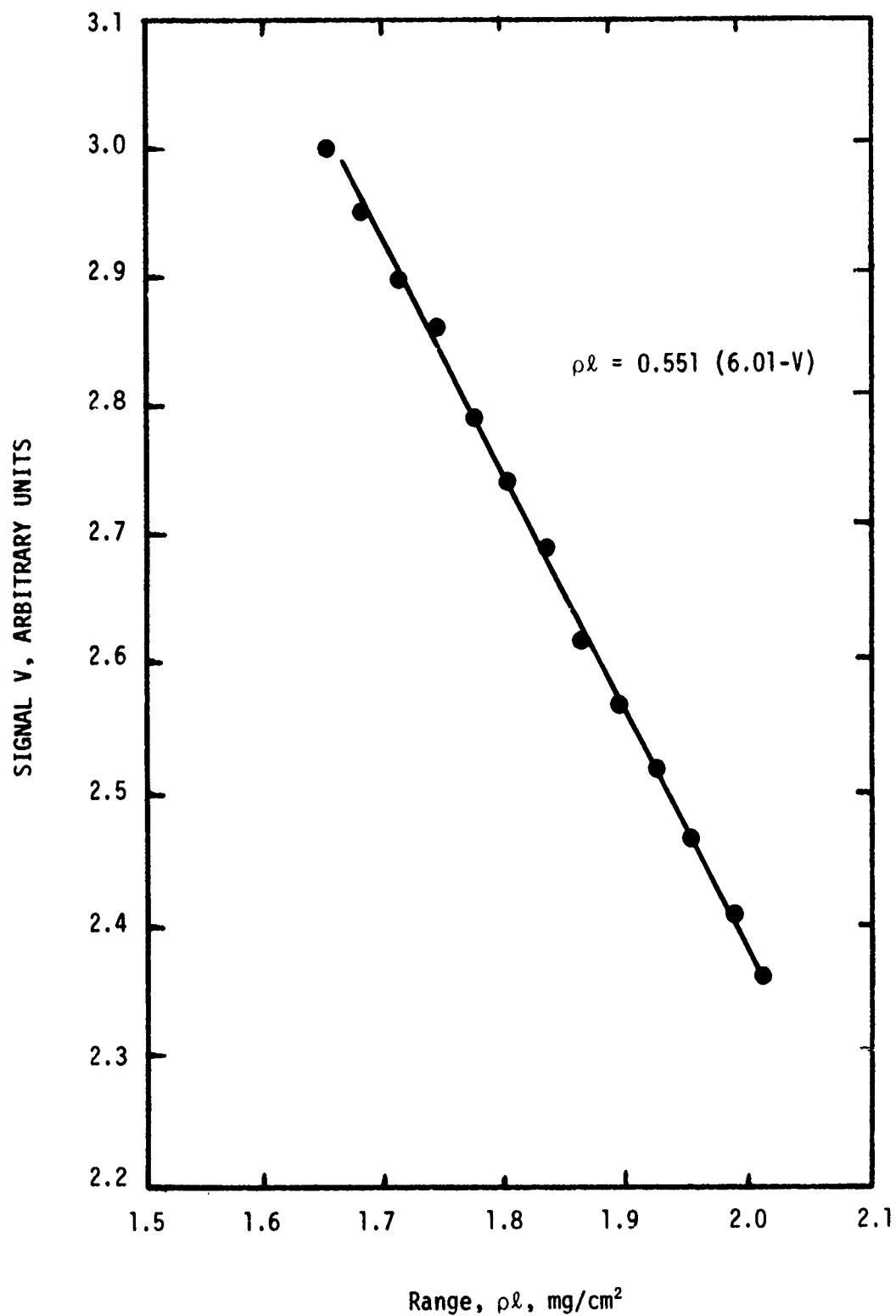


Figure 21. Range versus signal for the case #3 calibration.

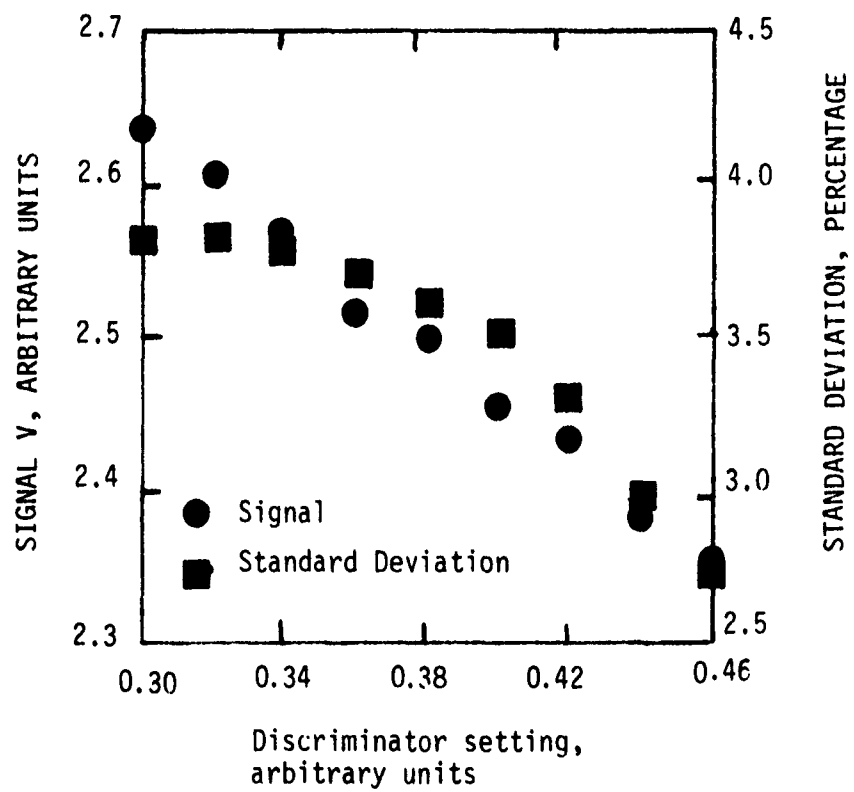


Figure 22. Effect of the discriminator level setting on the signal.

3. The narrow dynamic range, which is limited by the shift registers, requires that the device be calibrated for each range of interest. In addition, a linear fit to the data appears to be adequate.

Path length variation calibrations were performed regularly. The micrometer adjustment on the probe permits changes in path length to 0.1 mm. One such calibration is shown in figure 23. The results are clearly similar to the calibrations performed at PMEL.

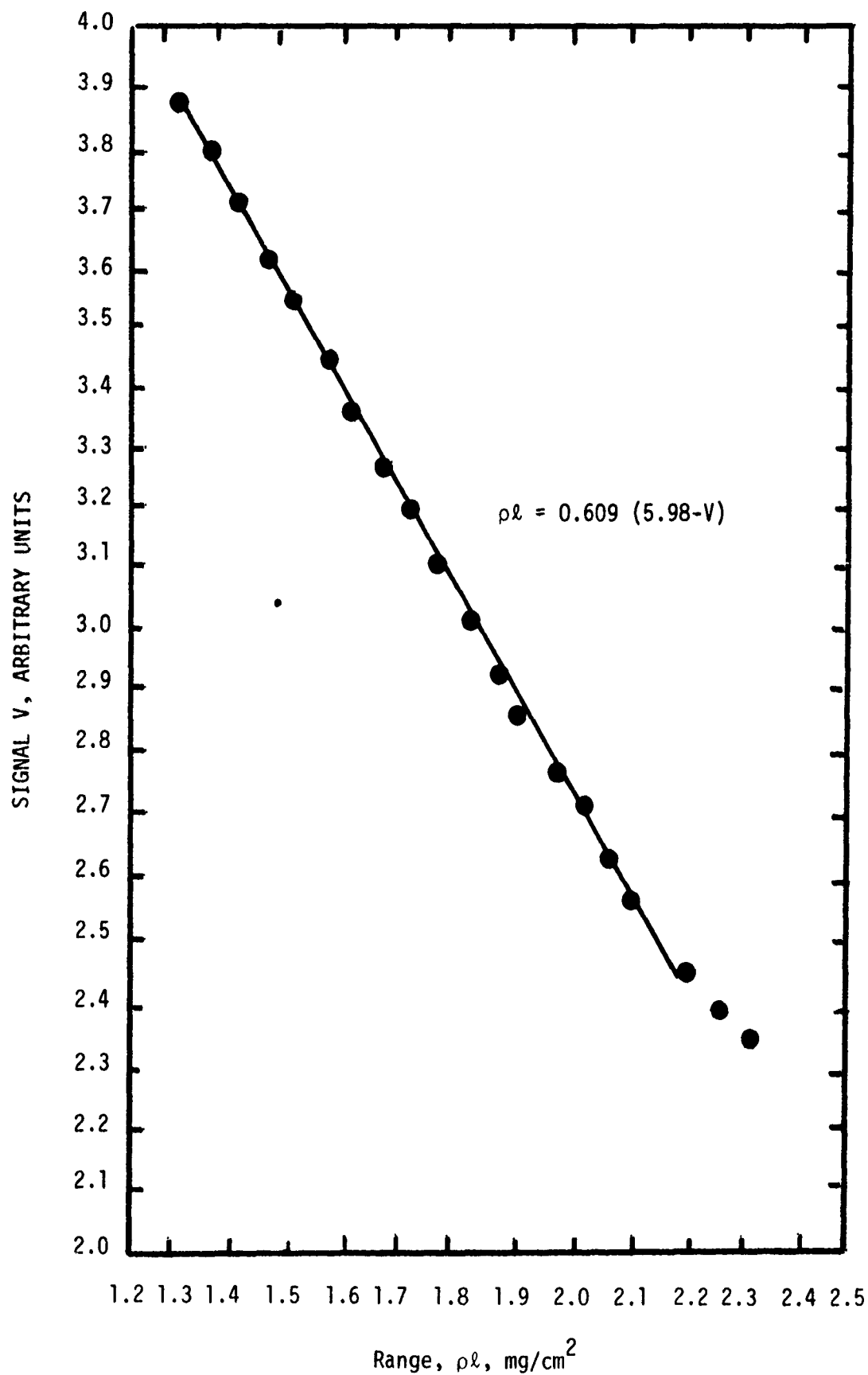


Figure 23. Range versus signal for varying path length calibration.

VIII. FREE CONVECTION DENSITY MEASUREMENTS

The results of Section VII demonstrate the ability of the probe to accomplish quasi-steady density measurements. The range of performance of the shift registers limits the range of the density measurement.

Also of interest is the demonstration of the measurement of a fluctuating flow of interest in which fluctuations are created by fluid flow and/or heat transfer. The frequency response is limited by the time for 64 counts to cycle through the shift registers. Free convection flow generated by a heated cylinder is one such flow field. The flow velocities generated by this condition are very low (a few cm/sec). Since the density measurement is virtually independent of flow velocity, it is not limited by this low velocity value as a hot-wire anemometer would be.

The density probe configured as in figures 7 and 8 was mounted such that the axis of the probe was 4.5 cm above the axis of a 1 cm diameter heated cylinder. The path length for this experiment was 2 cm and a calibration by varying the path length was accomplished. The probe was mounted on a transverse rack such that the path length aligns with the axis of the cylinder. The rack permitted horizontal positioning of the probe to within 0.1 mm. This permits the probe to be moved laterally in and out of the wake. The results of the measurements are shown in figure 24. The probe was moved laterally in increments of 2 mm except for near the edge of the cylinder where three measurements 1 mm apart were taken. With the exception of the density value at 3 mm the data are as expected. Each data point represents two data

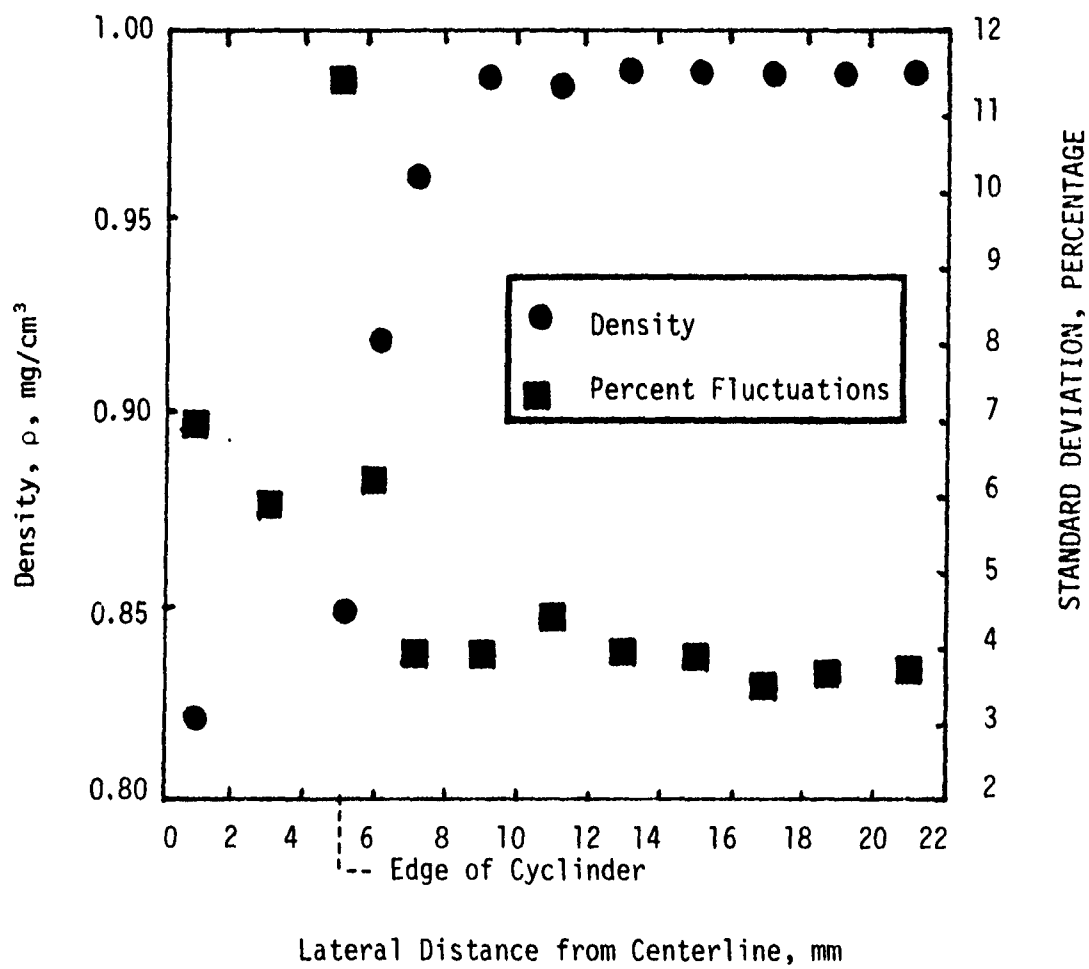


Figure 24. Mean density and percent fluctuations behind a heated cylinder.

sets. The fluctuations in density at the edge of the cylinder are relatively high, as expected. These fluctuations are not only caused by the density gradient but also by the slight lateral motion of the jet due to disturbances within the room. The data far from the edge of the cylinder show a fluctuation level of nearly 4% as opposed to the 1 to 2% level obtained in other calibrations. One cause for the greater noise is that the standard Ortec detector used here has a greater inherent noise level. Another possibility for this error is that the exit hole of the detector is 2 mm in diameter instead of 1 mm for the custom-built device. The sampling volume is therefore 2 mm in diameter and 2 cm long.

These test results clearly demonstrate the ability of the probe to measure density in a fluctuating flow field. The noise level is, however, slightly higher than desirable. These tests were performed in a quiescent, closed room with no ventilation. Another set of tests were attempted with a larger diameter heated cylinder, but they proved unsuccessful. In the next section of this report, the results obtained in a free-jet are presented and discussed.

IX. HEATED FREE-JET DENSITY FLUCTUATION MEASUREMENTS

In order to demonstrate the density probe in a flowing gas with density fluctuations, series of experiments were performed in a heated free-jet. In these series of experiments, a constant current wire anemometer operated in a unheated mode was also used to compare with the density probe performance.

The experimental configuration is shown in figure 25. Shown on the right is a standard laboratory heat gun with a 1.5 cm exit orifice. A three-position switch on the gun permits the generation of a heated or an unheated jet of air. The density probe and the anemometer were mounted 45 cm (30 nozzle diameters) downstream of the jet and about 3 cm off the jet centerline. Here the jet velocity was estimated to be 10 m/s. The jet temperature was measured with a standard laboratory mercury thermometer and found to be 53°C, which was 29°C above the ambient temperature.

Further detail of the measurement station is shown in figure 26. Here the direction of the flow is from right to left. Both instruments are mounted at the same height with the anemometer being halfway between the source and the detector and slightly downstream of the measuring path. At this location it will not interfere with the alpha particles. The path length between the detector and the source is approximately 2 cm. Note that the larger diameter Ortec detector was used here, since none of the microdetectors were operable when these tests were performed.

The anemometer was operated in an unheated mode so that it sensed the total temperature fluctuations. Since the jet is unconfined and its velocity low, these measurements corresponded directly to density fluctuations

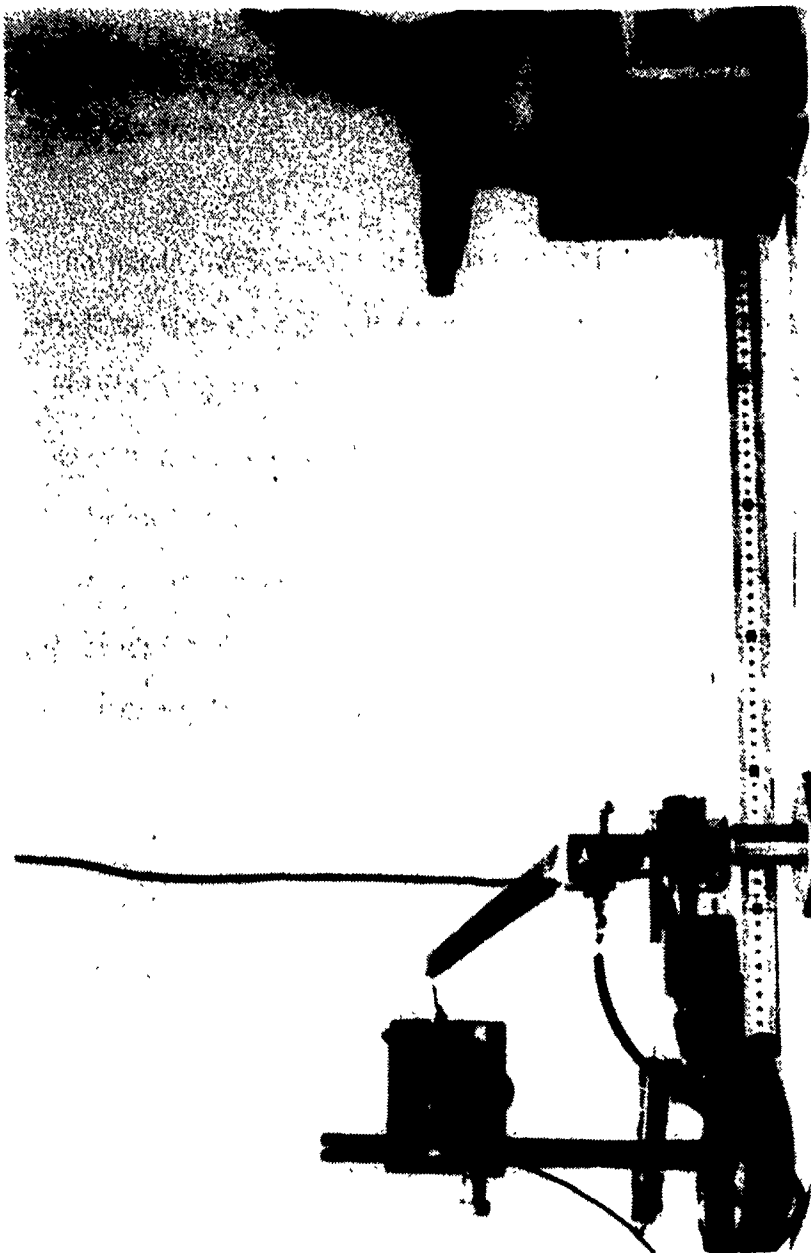


Figure 25. Heated free-jet equipment.



Figure 26. Detail of the probe/hot-wire configuration.

within the jet. The density probe provides a time-resolved density measurement (a new sample every millisecond), and hence the two measurements can be compared.

A series of measurements were performed with these instruments in order to characterize the flow and compare performance. The well-developed technology of the anemometer provided for an excellent data base by comparison. The spectra of the density fluctuations, as determined with the AFWL PDP 11/10 data acquisition system and the aid of AFWL personnel, indicated that the frequency of the fluctuations was primarily less than 500 Hz. This suggests that the strength of the source currently in use is adequate, since it is capable of delivering 64 counts in about 1 msec.

The anemometer measurements were accomplished by Dr. William C. Rose of Rose Engineering and Research, Inc., Incline Village, Nevada. The anemometer exhibited excellent signal-to-noise ratio for the measurements undertaken. Ambient air rms fluctuations were on the order of 0.006 volt. Cold jet rms fluctuations were on the order of 0.04 volt and heated jet rms fluctuations on the order of 0.68 volt. The sensitivity of the anemometer was $0.16 \text{ V}/^{\circ}\text{C}$. The density probe system, on the other hand, exhibited a rather poor signal-to-noise ratio 0.20 Vrms ambient, 0.21 Vrms cold jet and 0.28 Vrms heated jet, and sensitivity of 3.47 V/mg/cm^3 . The noisy signal is chiefly attributed to the signal processing equipment. This includes the preamplifier, shift register circuitry and the output summing amplifier. The Vrms reported here was measured by a DISA true rms meter for both the anemometer and the density probe. For the density probe, the output of the analog system was connected directly to the DISA true rms meter. The density probe and the anemometer produce voltage which are proportional to the density fluctuations in the range of interest here.

A calibration using the path length variation technique was accomplished for density probe for the DISA/PDP equipment and the data acquisition system (DAS) described in section 6. The calibration equations were found to be:

$$\rho l = 0.288 (11.34 - V) \quad (\text{DISA/PDP}) \quad (25)$$

$$\text{and} \quad \left| \frac{\Delta \rho}{\rho} \right| = \frac{1}{11.34 - V} \left| \frac{\Delta V}{V} \right| \quad (26)$$

$$\rho l = 0.680 (5.49 - V) \quad (\text{DAS}) \quad (27)$$

$$\text{and} \quad \left| \frac{\Delta \rho}{\rho} \right| = \frac{1}{5.49 - V} \left| \frac{\Delta V}{V} \right| \quad (28)$$

The value for V in these equations is dependent upon the recording system used.

A summary of the state variables are given in table 3. Pressure was not measured within the jet, but since it is unconfined and the velocity of the jet is low, it was assumed to be equal to ambient.

Table 3. State variable summary for jet conditions. Ambient pressure 0.085 MPa.

Condition	Measure Temperature (°C)	Computed Density (mg/cm ³)
Ambient	24	1.00
Cold Jet	26	0.993
Heated Jet	53	0.911

Table 4. Summary of free-jet data.

Condition	Quantity	Anemometer	Density Probe
Ambient	$\bar{\rho}$		1.00
Ambient	$\langle \rho' \rangle / \bar{\rho}$	0.013%	3.52%
Cold Jet	$\bar{\rho}$		0.995
Cold Jet	$\langle \rho' \rangle / \bar{\rho}$	0.08%	3.53%
Heated Jet	$\bar{\rho}$		0.908
Heated Jet	$\langle \rho' \rangle / \bar{\rho}$	1.42%	4.55%(2.36%)
Ambient	$\bar{\rho}$		0.997
Ambient	$\sigma / \bar{\rho}$		3.60%
Heated Jet	$\bar{\rho}$		0.913
Heated Jet	$\sigma / \bar{\rho}$		4.65%(2.94%)

Note: Values are explained in further detail within the text. The path length for the density probe was 1.885 cm.

Table 4 gives a summary of the data taken with the anemometer and the density probe. The anemometer data for the cold jet and heated jet is as reported in reference 4. The ambient condition for the anemometer was deduced from information contained in reference 4. The density probe data contained in the first six rows of the table were deduced from equations (25) and (26) and using the DISA averaging equipment. The density probe data contained in the next four rows were determined from the data acquisition system. Equation (27) is computed by this system, and the values in table 4 were directly displayed on the front panel. Density probe data represent the average over 3 separate test runs.

The measurement of density fluctuations with the DISA equipment results in the display of an AC coupled true rms value. The data acquisition equipment, on the other hand, computes the standard deviation. These two quantities are slightly different. The standard deviation is $n/(n-1)$ times larger than the AC coupled rms value, where n is the number of samples in the interval. In these experiments n is very large (at least 4096), and hence the values are essentially the same.

The values in parentheses in table 4 were computed by subtracting the noise at ambient conditions from the heated jet values. Assuming white noise, this is accomplished as follows:

$$\langle V'_s \rangle^2 = \langle V'_t \rangle^2 - \langle V'_n \rangle^2 \quad (\text{DISA}) \quad (29)$$

$$\sigma_s^2 = \sigma_t^2 - \sigma_n^2 \quad (\text{DAS}) \quad (30)$$

Where the subscripts s , t , and n refer to the actual signal, total and ambient values, respectively. The actual voltage rms values were used to compute the result with the DISA equipment, while the displayed standard deviations were used for the data acquisition system.

The fluctuations measured by the anemometer in the heated jet are of the order which is typically encountered in subsonic shear layers on aircraft. The signal-to-noise ratio for these levels of fluctuations is rather poor for the density probe system and thus the values deduced from equations (29) and (30) are of limited use. This is principally attributed to the inherent noise within the analog system. For example, the preamplifier exhibits a rather low signal-to-noise ratio (4 or less) and the interfacing between the shift registers themselves and to the summing amplifier is not perfectly mated. There also appears to be slightly more noise in the data acquisition system as compared to the DISA equipment.

The measurement of average density over a long time period, however, is quite good (less than 0.5%). There is no counterpart of this measurement with the anemometer system.

In the case of the DISA equipment this average was determined over several seconds. Within the data acquisition system, it represents the average of 4096 64-count sums taken over a period of about 5 seconds. In this case, the measurement is event dependent. The uncertainty in the ambient density from one 64-count sum measurement to the next is characterized by the standard deviation. In this case, the standard deviation is about 0.35 mg/cm^3 (3.5%).

The length scales of the turbulence in these measurements are also of interest. Measurements with two anemometers indicated that substantial coherence is lost at a separation distance of 14 mm. One expects the scale of density fluctuations to also be of this order. The density probe path length is on the order of 2 cm, and one would therefore expect spatial averaging over the length scales of interest. The resulting measurement should yield fluctuations lower than those indicated by the anemometer. Even after the noise is differenced, however, the fluctuations computed from the density probe are greater than those recorded by the anemometer. Due to the poor signal-to-noise ratio of the anemometer, it is difficult to draw any conclusion from the apparently anomalous result.

X. CONCLUSIONS

A compact density probe coupled within a high speed analog summing circuit and a high-speed digital data acquisition system has been demonstrated. Several new and unique components have been developed and demonstrated as a result of this effort. Several of the fundamental technological problems have been solved, leading the way for a refined probe system development.

A new microdetector was developed by Ortec, Inc. Its 1 mm active diameter and 3 mm OD presents the limiting minimum size for this technology. A compact 20 mCi source of the same diameter as the detector was developed by Isotope Products, Inc. It is not clear whether this is a limiting dimension, but, in light of the detector limit, there appears to be no reason to make the source smaller. Its size is most likely limited by internal heating and self-absorption. The half-life of polonium 210 (189 days) is a longevity problem, and some consideration should be given to americium 241 (475 year half life).

The analog system is the integration of several new systems. The high-speed preamplifier system represents new technology and was required so that counts could be rapidly measured. There is room for improvement in this device, however, both in the decay time and in the signal-to-noise ratio. The use of the analog shift registers for storing the energies of individual counts, provided a rapid, compact and low-cost measure for determining the mean residual energy over the 64 counts.

The measurements taken with the probe in both the free and forced convection environments, clearly demonstrate the ability and accuracy of the probe to measure mean density. The measurement of density fluctuations is suspect, however, principally due to the noise generated by the analog system.

REFERENCES

1. Golobic, R. A. and W. J. Honea, "Fundamental Experiments of the Alpha Particle Emitter Probe for Time-Resolved Density Measurements in the Air," Final Report, AFWL Contract F29601-77-C-0067, 12 December 1977.
2. Golobic, R. A. and W. J. Honea, "Analysis and Experiment of An Alpha Particle Emitter Probe Capable of Direct Air Density Measurements," AIAA paper no. 78-1199, presented at the AIAA 11th Fluid and Plasma Dynamics Conference, Seattle, WA, 10-12 July 1978.
3. Friedlander, G., J. W. Kennedy, and J. M. Miller, Nuclear and Radiochemistry, 2nd edition, John Wiley, 1964, Chapter 4.

GLOSSARY

<u>SYMBOL</u>	<u>DEFINITION</u>
A	Constant, cf equation (6)
b	Constant, cf equation (6)
B	Constant, cf equation (3)
D	Constant, cf equation (3)
E	Alpha particle energy
E_0	Initial alpha particle energy at source
E_r	Residual alpha particle energy at detector
l	Path length from source to detector
M_∞	Free stream Mach number
N	Total number of counts in a sample
P	Absolute pressure
T	Static temperature
V	Output of data acquisition system, corresponds to E_r , cf equation (21)
σ	Standard deviation
ρ	Density
< >	rms value

DISTRIBUTION

USAF, Wash	Centennial Sci Inc, Colorado Springs
(INAKA)	AFWL
(TACGS)	(SUL)
AFSC	(ARLB)
(XRLW)	(ARL)
(DLWM)	(ARL-2)
SD/DYV, Los Angeles	(ARE)
AFWAL	(ARA)
(CA)	(ARAA)
(AART)	(ARLO)
(WRW)	(ARLI)
ESD/XRE, Bedford	(ARLD)
AFFTD/ETDB	(ARLB)
6585 Test Gp/GDA	(ARAO)
AUL/LDE	(HO)
DTIC/DDA, Alexandria	(MRAT/PO)
USA Msl Rsch & Dev Cmd,	Official Record Copy (AFWL/ARLB/Capt
(DRCPM-HEL)	deJonckheere)
(DRCPM-HEL-P)	
(DRCPM-HEL-S)	
Bal Msl Def Tech Cen/ATC-D, Huntsville	
Off of NAV Rsch, Boston	
Off of NAV Rsch, Arlington	
NAV Rsch Lab, Wash	
NAV Ord Sys Cmd/PMS, Wash	
DARPA, Arlington	
(DCP)	
(STO)	
DIA/DT-1A, Wash	
Aerospace Corp, Los Angeles	
AVCO Everett Rsch Lab, Everett	
Boeing, Seattle	
C. S. Draper Lab, Cambridge	
Env Rsch Inst of MI/IRIA Lib, Ann Arbor	
Ford Aero & Comm Corp, Newport Beach	
BDM Corp, Albuquerque	
United Tech Rsch Cen, East Hartford	
AFELM/Rand Corp, Santa Monica	
Optical Sci Consultants, Placentia	
Perkin-Elmer Corp, Norwalk	
P&W Aircraft, West Palm Beach	
Gen Dyn, San Diego	
Hughes Aircraft Co, Culver City	
Johns Hopkins Univ Applied Phys Lab, Laurel	
Lockheed Msl & Space Co, Sunnyvale	
Lockheed Msl & Space Co, Albuquerque	
McDonnell Douglas Astro Co, Huntington Beach	
Sci Appli Inc, Albuquerque	
NAV Post School, Monterey	
Rose Engr & Rsch Inc, Incline Village	
Spec Dev Labs Inc, Costa Mesa	